โครงการ

การเรียนการสอนเพื่อเสริมประสบการณ์

ชื่อโครงการ การศึกษาความผันผวนของคลื่นไมโครเวฟพื้นหลังของจักรวาลในเชิงสถิติ
Study of the Statistics of Cosmic Microwave Background Fluctuations

ชื่อนิสิต นายชนสรณ์ คงปรัชญา **เลขประจำตัว** 6033408623

ภาควิชา ฟิสิกส์

ปีการศึกษา 2563

คณะวิทยาศาสตร์ จุฬาลงกรณ์มหาวิทยาลัย

Study of the Statistics of Cosmic Microwave Background Fluctuations

Chanasorn Kongprachaya

Department of Physics, Faculty of Science
Chulalongkorn University

Submitted in partial fulfillment of the requirements for the degree of Bachelor of Science in
Department of Physics, Faculty of Science, Chulalongkorn University
Academic Year 2020

APPROVAL SHEET

Project Title	Study of the Statistics of Cosmic Microwave Background Fluctuations
By	Chanasorn Kongprachaya
Department	Department of Physics
Academic Year	2020
Advisor	Asst. Prof. Dr. Pawin Ittisamai
Co-advisor	Dr. Spyros Sypsas

This report has been approved by the committee:

Name	**Signature**	**Date**
Asst. Prof. Dr. Burin Asavapibhop (**Chairman**)		25 May 2021
Asst. Prof. Dr. Auttakit Chatrabhuti (**Committee**)		25 May 2021
Asst. Prof. Dr. Pawin Ittisamai (**Advisor**)		25 May 2021
Dr. Spyros Sypsas (**Co-Advisor**)		25 May 2021

Abstract

Observations of *Cosmic Microwave Background* (CMB), radiation created shortly after the Big Bang and presents almost uniformly across the universe, are our most important information about relevant physics during the beginning of our universe. The slight variations in the temperature of CMB provide evidence for testing predictions from models of the very early phase. Arguably, one of the best candidate models of the very early universe is *inflation*, a period of exponential expansion. In this project, we review how the quantum fluctuation in this era seeds the CMB pattern. We study the implications of the non-Gaussianity profile of CMB temperature fluctuation on the physical aspect of inflationary models. We calculate correlation functions that allow comparison with observations to constrain non-linear parameters of the non-Gaussianity under a power-series ansatz. Then, we discuss single-field consistency relation which shows how detecting a large three-point function could eliminate all single-field inflationary models of inflation. We also discuss multi-field consistency relations where a weak signal of a four-point function compared to the two-point function could rule out a large class of multi-field models. Finally, we mention the limitations of this approach.

Acknowledgements

I cannot express enough thanks to my co-advisor, Dr. Spyros Sypsas, for useful and constructive guidance during the planning and development of this project. His willingness to give time so generously has been very much appreciated. Secondly, I would like to express my very great appreciation to my advisor, Asst. Prof. Dr. Pawin Ittisamai, for the encouragement and useful critiques. His recommendations and comments are more than helpful to this research work. Next, I would like to thank the CUniverse research promotion for the invaluable opportunity to have a fruitful discussion with fellow researchers. Also, I'm very grateful to be a part of the Group Study for Undergraduate Student (GSUS). The group creates an energetic and encouraging environment to study beyond the standard curriculum, which is very beneficial for this project. Finally, I'm very thankful for my family and friends for always be supportive during the preparation of this project.

Contents

1. Introduction

One of the main goals in cosmology is to explain the evolution of the universe. Nowadays, several things about it have been explained. For example, it is expanding [1, 2]. This came from the fact that light from distant sources redshifts. This phenomenon is called cosmological redshift. That is, the expansion stretches the wavelength of light. Another thing that we know is the universe is homogeneous and isotropic at a large scale. This led us to the standard universe model based on Einstein's theory of gravity: general relativity. However, there are also many things that have not been concluded until now. For instance, no one has confirmed how the universe was born or how physics works at the very beginning. Presently, we can only make just a few descriptions of it. One of the reasonable assumptions is it should be very tight. This is because the expansion is so well-observed, therefore the starting point should be much smaller than nowadays. Also, the energy density should be much higher than the present time due to tiny space. This makes the particles at that time have very high energy, much higher than the binding energy of the atom. Hence, they are not bound to one another and can travel freely. To be precise, those free particles are independent charged particles. Thus, they spontaneously interact with each other all the time via electromagnetic interaction. This group of impulsively interacting particles is also known as the primordial plasma or the particle soup. After the universe expands out and cools down, the particles stopped spontaneously interacting and became bound with one another. This is the time when hydrogen atoms are formed, also known as *Recombination* [3]. Those inert atoms and particles become relics which later form stars and other cosmic objects that we observed nowadays.

Apart from the explanation above, there are still many problems that await to be answered. In the past decades, one of the hot topics is the physics before the existence of those particles mentioned earlier, the standard model's particles. This topic motivates by the fact that we could discover some new physics that cannot be detected in the present environment. As mentioned, the energy scale in the past is much higher than these days. This could allow new phenomena to emerge due to the energetic environment. Until now, the matter component that governed the very early universe remains unknown. By studying it thoroughly, we might reveal some new particles and interactions that only appear at high temperature, and possibly the origin of the standard model's particles. This is similar to the objectives of the particle colliders. There, the particles are accelerated to make intense collisions, which show us signatures of new physics that only appear in a high energy scenario. For example, the particle that carries the weak interaction, *W boson*, was discovered by this method. Here, the idea is quite the same. The observation in this study is the *Cosmic Microwave Background* (CMB) radiation. As we are going to explain later, this radiation is the oldest signal that we can observe, which is coded with signatures created by the behaviour of the matter at a very early time. Thus, it is equivalent to a picture of a collision event, whose energy is much higher than the particle accelerator. Thus, it is an alternative source of studying high energy physics. In this project, we will focus on the study of the very early universe via possible observations.

As recently mentioned, the oldest evidence that we can observe nowadays is CMB. This is the first light emitted around 13.7 billion years ago. As mention before, the charged particles (protons and electrons) form hydrogen atoms after the universe cooled down enough which are overall neutral charged. Since electromagnetic wave interacts with charged particles only, it hardly interacts with hydrogen atoms (just a few with specific wavelength are absorbed and emitted by the atom). The universe then becomes transparent in this period. That is, photons roam freely throughout the space. Presently, the radiation that reaches the Earth can be observed in the sky as CMB. The cosmological surveys [4–7] can measure the energy or the wavelength of it, which represented by the background temperature from which the CMB was emitted. This is possible because the temperature of an object can be determined from the wavelength of the radiation emitted from it via the theory of black-body

radiation.

As noted, CMB was emitted when hydrogen atoms are formed. In this context, we can measure the temperature at the point of recombination. The surveys show that the temperature is almost uniform throughout the sky, fluctuates within the order of 10^{-5} compared to its average magnitude. As we are going to discuss later, they were induced by the primordial curvature fluctuations of space-time. These disturbances cause an uneven gravitational redshift to the CMB, which results in a small temperature difference among each point. This makes the CMB map a perfect snapshot of the space-time disturbances at an early time. Furthermore, these fluctuations also seed the structure formation of the universe like galaxies and stars. By understanding it thoroughly, we'll be able to describe the origin of the universe structure as well, and vice versa. Also, the study can give us some hint about primordial matter. This is because Einstein's theory of general relativity tells us that space-time is curved by matter. Thus, these primordial curvature fluctuations must be created by the matter component existed in a very early time. This overall makes CMB a suitable object to learn about primordial physics. Nowadays, recent analyses can extract out only the temperature fluctuations created by primordial matter.

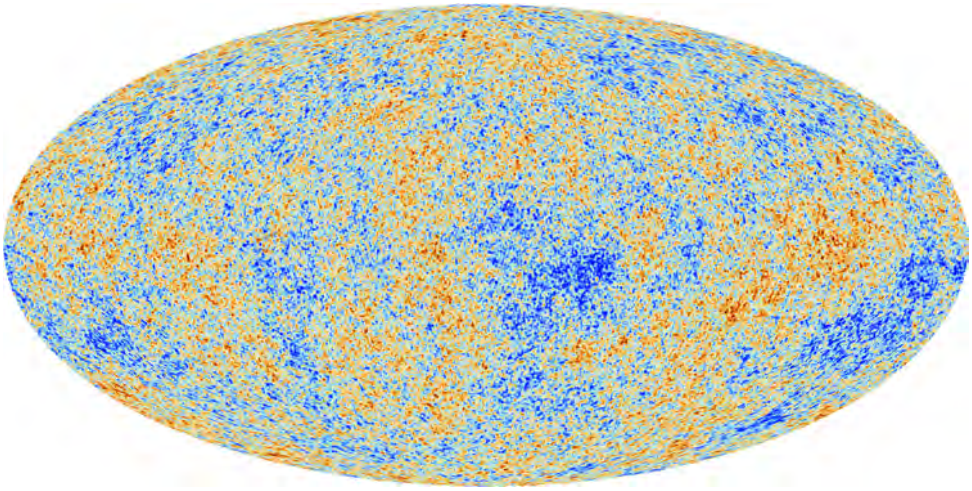

Figure 1: Picture of the CMB map captured by the Planck satellite [4]. From this survey, the average temperature is around 2.7 Kelvin. The points with a temperature higher than average are represented with warm colours, and the cooler spots are represented with cold colours. The average magnitude of the fluctuation is around 10^{-5} *of its average temperature.*

To study the very early universe via observations, one should start by choosing a model of the very early universe that can explain the CMB. This is because we will need some relations between the CMB fluctuations and the primordial matter first. One of the well-established models is *inflation*: a period of rapid, exponential expansion [8–12]. It is a suitable model for the reason that it provide solutions to many problems. Just to mention one of those problems, the *Horizon problem* is about the causality of the CMB. As we are going to discuss later, inflation solved this problem with its rapid expansion. Next, the character of inflation also implies some aspects of the matter that existed during this period. Since the observations told us that the universe is homogeneous and isotropic on a large scale, it should be the same for the period of inflation as well. This is because the large-scale structure of the universe expanded from a tiny space of inflation. The assumption leads to a homogeneous scalar field of inflation called *inflaton*, which is the simplest model. A scalar field itself has no preferred direction. Thus, a homogeneous scalar field fits very well with these aspects. Also, inflation can predict the form of the CMB from the characteristic properties of the model as follows. Since inflation started from a very tiny space, quantum mechanics must play an important role [13–16]. Therefore, the field should be probabilistic and statistically distributed rather than a single deterministic value. This creates the field fluctuation that seeds the CMB as mention before. In this context, The form of the field's Lagrangian can tell us how the quantum fluctuations are

distributed. For example, a quadratic action implies Gaussian distributed fluctuation. For inflaton, the action contains a potential term that can be non-quadratic. As we are going to explain later, the accelerated expansion is driven by potential energy. Thus, the declination of potential energy slows down the expansion. To maintain the exponential expansion throughout inflation, we demand a flat potential compared to the evolution of the field. Therefore, the potential term will have just a little effect on the evolution of field fluctuations, thus can be neglected from the action. This made the distribution of the field fluctuations approximately Gaussian for this simplest model of inflation.

However, the actual model does not have to be the simplest. Although the latest observation reveals that CMB statistics are close to Gaussian distribution, the measurement still has uncertainty. Thus, there is a chance that the distribution is not exactly Gaussian [17]. This is motivated by the fact that there are possible features beyond the simplest model that can produce non-Gaussianity. Also, we expect the theory to be more complicated on a high energy scale as already mentioned in the first paragraph. The study indeed shows that there are some scenarios where the distribution becomes non-Gaussian [18–27], e.g. multi-field inflation (see section 5), which will be discussed later in this project. Here, the non-Gaussian signatures could tell us more about the physics of the very early universe which produces those non-Gaussianities. For instance, the result of this study might reveal some new particle species and their behaviour. Moreover, this also provides us with the initial condition for structure formation like stars and galaxies as mentioned. In summary, a well-measured CMB temperature map could give us some clues and narrow down the group of the inflationary model candidates.

In section 2, the standard expanding universe model is recalled to give some background of our universe in general. Section 3 will look back on some motivations for the inflationary model. Also, the simplest model of inflation will be introduced. Then, section 4 is going to explain how inflation can gives the initial condition to the present universe. This will link the primordial fluctuations to the CMB temperature fluctuations and we will end the section with the statistics given by the simplest model. Section 5 initiates the analysis of non-Gaussianity. Here, we will argue that the statistical moments must be computed in order to reveal the actual statistics. Subsequently, section 6 and 7 will show some aspects of the inflationary model that we can learn from the computed moments. Lastly, the future of this study will be informed in section 8.

2. Geometry of Expanding Universe

As mentioned, observations found that light from a distant object redshifts. This is concluded to the expanding behaviour of the universe that stretched out the wavelength of light. To be precise, we can exclude this phenomenon from Doppler and gravitational redshift for the following reason. By observing a distant object, the light of it is dimmer while the object appeared bigger than expected. This happens only if the universe is expanding since the expansion will spread out the intensity and magnify the appearance of the object. This section will review the geometry of the expanding universe for further discussion about inflation and more.

From the theory of general relativity, the geometry of space-time and the matter on it related to each other via the Einstein Field Equation:

$$G_{\mu\nu} = 8\pi G T_{\mu\nu}, \tag{2.0.1}$$

where $G_{\mu\nu}$ is the Einstein tensor and $T_{\mu\nu}$ is the energy-momentum tensor. Here, we use the convention: $c \equiv 1$ for convenience. Briefly speaking, $G_{\mu\nu}$ is taking account of the space-time structure while $T_{\mu\nu}$ on another side represent matter on it. The word "geometry" here refers to the thing that regulates the trajectory of an inertial particle. The geometry will tell matter how to move along its curve and the matter will also curve the geometry of the space-time. On the geometry side, the distance on the space-time, the line element, is written as

$$ds^2 = g_{\mu\nu} dx^\mu dx^\nu \tag{2.0.2}$$

where $g_{\mu\nu}$ is the metric tensor. For our universe, the metric tensor must respect the observed isotropy and homogeneity of the background. Thus, the tensor is position-independent and direction-independent. Also, the spatial distance grows with time since the universe is expanding. Therefore the metric takes the ansatz

$$g_{\mu\nu} = \begin{pmatrix} 1 & 0 & 0 & 0 \\ 0 & -a^2(t) & 0 & 0 \\ 0 & 0 & -a^2(t) & 0 \\ 0 & 0 & 0 & -a^2(t) \end{pmatrix} \tag{2.0.3}$$

and the line element takes the form

$$ds^2 = dt^2 - a^2(t)\delta_{ij} dx^i dx^j. \tag{2.0.4}$$

The scale factor $a(t)$ is introduced as an amount of expansion depend on time. This causes the physical coordinates to expand compared to static coordinates (which we are going to refer it as *comoving coordinates*). This is called the Friedmann-Lemaître-Robertson-Walker metric (FLRW metric). The metric presents the geometry of the universe which directly affect the trajectory of a particle on space-time. To explain how matter affects the rate of expansion, one can load the FLRW metric into the Einstein field equation and gets the *Friedmann equations*,

$$H^2 = \frac{\rho}{3M_{pl}^2} \tag{2.0.5}$$

$$\dot{H} = -\frac{\rho + P}{2M_{pl}^2}. \tag{2.0.6}$$

The constant M_{pl} is the Planck mass. The variables ρ and P are the energy density and the pressure

of matter, respectively. The Hubble parameter H is introduced to represent the expanding rate of the scale factor compared to its magnitude defined as $H \equiv \frac{\dot{a}}{a}$. These are basic ideas of the expanding universe model (FLRW universe) which explains the universe's history. The following section will discuss its early evolution, which is the main topic of this project.

3. Inflation

As noted in the introduction, there are many problems in the standard cosmological model. This leads to several proposals of the very early universe model with the hope to resolve them. One of the models is *inflation* [8–12], which is a period of rapid expansion. This characteristic property of this model succeeds in explaining many of those issues, one of them is the *Horizon problem*. To give an example of why inflation is a suitable model, the subsequent subsection will show the explanation of the Horizon problem given by it.

3.1. The Horizon Problem

As mentioned in the introduction, by the time the universe has cooled down enough to form hydrogen atoms, photons decoupled from the primordial plasma. Those hot photons travel through the universe and redshift due to the universe's expansion. Finally, those photons reached us as microwave radiation. This is the Cosmic Microwave Background (CMB) radiation, the first light emitted in the early universe. The measurements show that the CMB temperature is quite uniform (with tiny fluctuations around 10^{-5} of its average magnitude). This suggests that every point on the CMB should be in causal contact with each other in the lifetime of the universe. This causes a serious problem since there would not be enough time for every point in the sky to contact each other before. If we based on the observed matter content, the expansion of the universe computed via the Friedmann equations (2.0.5,2.0.6) would not be fast enough to become the CMB map this big. Thus, inflation is proposed as a period of accelerated expansion in the very early universe to resolve this problem. This rapid expansion stretched out the primordial background from a tiny point to the size of the observed sky in a brief time. Later, the stretched background creates a uniform temperature map with the size that we observe nowadays. This is why inflation is a well-established model. Every discussion about the physics of the very early universe in this project will be based on this model.

3.2. Condition for Inflation

There are some conditions to be satisfied for inflation to occur. For instance, inflation must maintain the accelerated expansion for a long enough time to solve the Horizon problem as discussed in the last subsection. The accelerated expansion condition, $\ddot{a} > 0$, can be written in terms of the Hubble parameter:

$$\epsilon \equiv -\frac{\dot{H}}{H^2} = -\frac{d\ln H}{dN} < 1, \tag{3.2.1}$$

where we have defined $N \equiv \ln a$ as the number of e-folds of expansion. Here, the parameter ϵ is defined to represent the rate of change of the Hubble parameter. This expression tells us that the accelerated expansion will at least require the parameter ϵ to be smaller than 1. Also, inflation must persist for a while in order to solve the problem. Namely, the condition should hold throughout inflation which will require ϵ to change slowly. Thus, we demand another condition to control the change of ϵ. To present it, a new parameter is defined:

$$\eta \equiv \frac{d\ln\epsilon}{dN} = \frac{\dot{\epsilon}}{H\epsilon}. \tag{3.2.2}$$

This parameter represents the rate of change of the parameter ϵ. Thus, it will require $|\eta| < 1$ to keep the parameter ϵ small. In summary, it will at least require $\epsilon, |\eta| < 1$ for inflation to occur. In

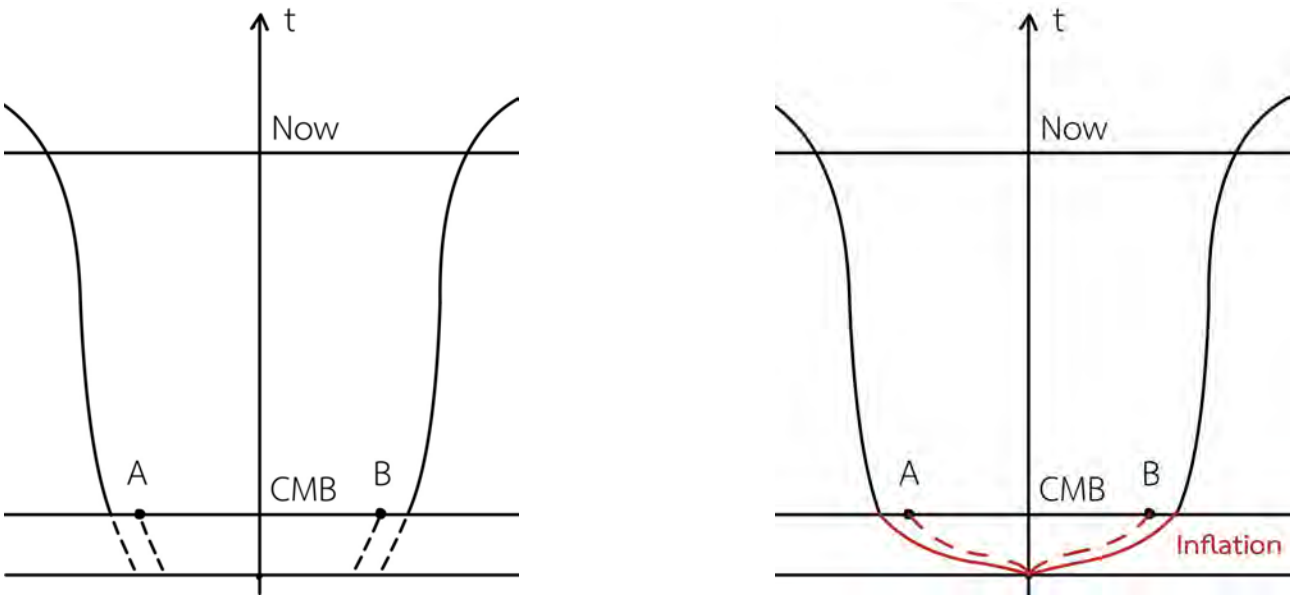

(a) The evolution without inflation.

(b) The evolution with inflation.

Figure 2: The solution to the horizon problem given by inflation. In (a), the points on CMB, A and B, were not connected before if we based on the expansion by the common matter content. In (b), inflation is included. The points A and B were connected before thanks to the exponential expansion driven in inflation.

general, we can introduce higher-derivative parameter for more accurate evolution [28]. But, it will be discussed further that we are interested in the period where these parameters are much smaller than 1. In this project, parameters of this kind thus can be kept up to linear order in every expressions and these two parameters will be enough to discuss the results in this expansion up to that order.

3.3. The de Sitter Expansion

For $\epsilon = 0$, the Hubble parameter is constant via the definition of ϵ. This often refers to perfect inflation where the expansion becomes exponential, which is the so-called *de Sitter expansion*. By solving for the scale factor in this condition, one finds that the scale factor grows exponentially. Therefore, the metric is written as

$$ds^2 = dt^2 - e^{2Ht}\delta_{ij}dx^i dx^j. \tag{3.3.1}$$

This is why inflation is often described as the period of exponential expansion. Keep in mind that it will not last forever. The parameter ϵ should be varied at least slowly to take inflation to an end. One might call it a *quasi-de Sitter expansion* since the expansion is not exactly de Sitter all the time. However, it is still a nice approximation when considering the period far from the end of inflation, which is where our main discussion is about. This expansion will be assumed when we compute the field fluctuations in inflation in subsection 4.3.

3.4. Conformal Metric

Before we continue to discuss the physics of inflation, it is convenient to introduce the conformal metric. It is defined such that both space and time are expanding together. Therefore, the angle of a distance in space-time preserved under the expansion. Thus, the metric is conformal and comoving with the expansion. This is a handy way of seeing things that evolve in the expanding universe since

we do not have to worry about the difference between the scale of time and space. This metric is written as

$$ds^2 = a^2(\tau)(d\tau^2 - \delta_{ij}dx^i dx^j). \tag{3.4.1}$$

Conformal time is introduced and defined as $d\tau \equiv \frac{dt}{a(t)}$. The original time scale t will be called *physical time* from now on. The Hubble parameter also changes its form in conformal time scale to

$$\mathcal{H} \equiv \frac{a'}{a}. \tag{3.4.2}$$

The primed parameter denotes the conformal time derivative of that parameter. This Hubble parameter in conformal time scale is related to the Hubble parameter in physical time scale such that $\mathcal{H} = aH$. In brief, the change of time scale will adjust the look of some equations but will not affect the physics of it whatsoever. For example, in conformal time, the scale factor of de Sitter expansion takes the form

$$a(\tau) \propto -\tau^{-1}. \tag{3.4.3}$$

Note that the conformal time has a negative value in inflation. This comes from the fact that the scale factor positively grows from zero, thus the domain of τ is pushed back to $-\infty$. Therefore, the conformal time domain in inflation is $(-\infty, 0]$. It is important to emphasize that this is just a convenient way to represent the geometry for simplicity of the equations. In this metric, the matter simply evolving on a expanding Minkowski space. In this project, the form will be adopted to explain the physics of inflation, i.e. the explanation about matter in inflation in the next subsection.

3.5. The Scalar Field

CMB is the evidence left by the primordial matter in inflation. To study the physics of inflation from the observations, one must investigate what kind of matter that drives inflation first. Then, some predictions can be computed and compared with the observations. Surveys show that CMB temperature is quite uniform throughout the sky and does not have any preferred direction. This suggests a homogeneous and isotropic background of the very early universe. Therefore, the inflation background should be governed by a scalar field, which is isotropic. Also, the scalar field should be position-independent to satisfies the homogeneity. This scalar field $\phi(t)$ is called *inflaton* which is the simplest model of inflation. Dynamics of this field on space-time is presented by its action, which is written as

$$S = \int d\tau d^3x \sqrt{-g}\Big[\frac{1}{2}g^{\mu\nu}\partial_\mu\phi\partial_\nu\phi - V(\phi)\Big], \tag{3.5.1}$$

where $V(\phi)$ is the potential term of this field and $g \equiv \det(g_{\mu\nu})$. Note that we use the conformal metric here. One can derive the equation of motion of the background scalar field via the Euler-Lagrange equation. By substituting the inflaton's Lagrangian into the equation, one finds that the equation of motion is the *Klein-Gordon equation*:

$$\phi'' + 2\mathcal{H}\phi' + a^2 V_{,\phi} = 0. \tag{3.5.2}$$

The expression $V_{,\phi} \equiv \frac{dV}{d\phi}$ is the derivative of the potential with respect to the field. From Noether's theorem, the symmetry of a Lagrangian corresponds to a conserved quantity. In this case, it is the energy-momentum tensor which is written as

$$T_{\mu\nu} = \partial_\mu\phi\partial_\nu\phi + g_{\mu\nu}\left(\frac{1}{2}g^{\alpha\beta}\partial_\alpha\phi\partial_\beta\phi - V(\phi)\right). \tag{3.5.3}$$

The indices of the energy-momentum tensor can be raised and lowered by the metric tensor. Since the field is homogeneous, the terms with the spatial derivative of the field vanish. The energy density

and the pressure in inflation can then be written as

$$\rho_\phi = T_0^0 = \frac{1}{2}\Big(\frac{\phi'}{a}\Big)^2 + V(\phi), \tag{3.5.4}$$

$$P_\phi = T_i^i = \frac{1}{2}\Big(\frac{\phi'}{a}\Big)^2 - V(\phi). \tag{3.5.5}$$

Here, we have got a simple background scalar field that represents the matter on space-time. Next, we are going to discuss the conditions of the scalar field that drives the rapid expansion.

3.6. Slow-Roll Inflation

Next, we are going to investigate the feature of the scalar field that drives inflation. One of the models that describe this period is the *slow-roll inflation*. This model sets conditions to the scalar field as follows. By substituting ρ_ϕ and P_ϕ into the Friedmann equation, one can see that the kinetic term induces a change of Hubble parameter and the total energy density is directly proportional to the square of Hubble parameter. In this model, the kinetic energy of the field must give a tiny contribution to the total energy. This will keep the Hubble parameter unchanged compared to its value so the field can generate a long enough inflation to solve to the Horizon problem. The condition here is presented by the small value of parameter ϵ:

$$\epsilon \equiv -\frac{\mathcal{H}'}{\mathcal{H}^2} = \frac{\frac{1}{2}\phi'^2}{M_{pl}^2\mathcal{H}^2} \sim \frac{\text{Kinetic energy}}{\rho_\phi}. \tag{3.6.1}$$

Furthermore, by substituting ϵ and its conformal time derivative into the definition of η in conformal time scale, one gets

$$\eta = 2\frac{\phi''}{\mathcal{H}\phi'} - 2\frac{\mathcal{H}'}{\mathcal{H}^2}. \tag{3.6.2}$$

ϵ and $|\eta|$ are called the *slow-roll parameters* from the fact that they represent the condition of the slow-roll inflation. In this model, those parameters are required to be much smaller than 1. Here, the Hubble parameter is hardly changed, which induced the approximately exponential expansion. This is the so-called *slow-roll approximation* where inflation occurs and persists with quasi-de Sitter expansion.

In another way, one can argue that the total energy density approximately equals potential term in slow-roll inflation. Therefore, the condition now is to keep the potential energy approximately constant compared to its own value. One can apply this approximation to the Klein-Gordon equation and get a new set of parameters:

$$\epsilon_V \equiv \frac{M_{pl}^2}{2}\Big(\frac{V_{,\phi}}{V}\Big)^2, \tag{3.6.3}$$

$$|\eta_V| \equiv M_{pl}^2\frac{|V_{,\phi\phi}|}{V}. \tag{3.6.4}$$

We have defined $V_{,\phi\phi} \equiv \frac{d^2V}{d\phi^2}$. These new parameters represent the change of the potential term to the field. The slow-roll potential requires $\epsilon_V \ll 1$ to keep the potential approximately constant and $|\eta_V| \ll 1$ to keep ϵ_V small. One must keep in mind that these parameters are not the same as the previous ϵ and η which are often called the *Hubble slow-roll parameters*. Those parameters are used to represent the condition that keeps the Hubble parameter changes slowly. But, the parameters ϵ_V and η_V are used to create the condition that keeps the potential approximately flat and hardly changed. These parameters are called the *Potential slow-roll parameters* which can judge if the given potential can lead to slow-roll inflation or not. These parameters can be related to each other as $\epsilon_V \approx \epsilon$ and $\eta_V \approx \epsilon - \frac{1}{2}\eta$ during slow-roll inflation. At this point, we have reviewed the important background

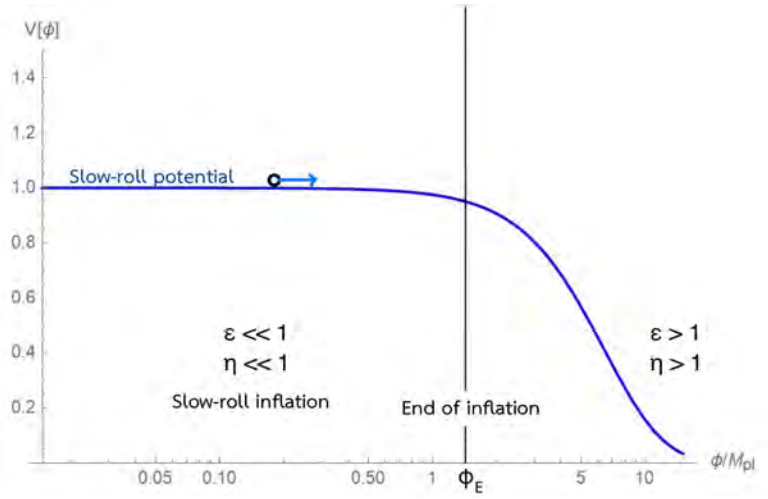

Figure 3: This is a broad illustration of the inflaton potential that drives the slow-roll inflation. In the context of slow-roll, the potential must be approximately flat to maintain an exponential expansion corresponding to small ϵ_V *and* η_V*.*

for our main discussion, the CMB. The subsequent section will use these descriptions to explain the mechanism that generates the form of CMB and how it is related to the aspect of inflation.

4. Initial Condition from Inflation

As already mentioned, the matter content in inflation seeds the CMB fluctuations and the structure formation. One may ask how it gives the initial condition such that it is produced the particular CMB pattern on the sky. From the last section, inflation is governed by the scalar field, the inflaton. Since inflation starts from a tiny region, the quantum behaviour of the field is significant. One could start by considering the quantum uncertainty of the field as a source of the CMB fluctuations. After inflation ended, the inflaton has to decay to the standard model's particle. In this period, the universe is heating up and subsequently enters the era called *Reheating* [29, 30]. Until now, there is no clear explanation about physics in this period. Hence, the evolution of the field fluctuations is unknown as well. Luckily, there is another way around. From the Einstein field equation, the fluctuations of the field will curve the space-time. Thus, they will create curvature disturbances. Unlike the field perturbations, they are conserved throughout the reheating. These curvature disturbances then cause gravitational redshift to CMB, results in temperature fluctuations. This section will show how the inflaton perturbations are related to the CMB.

We are going to start with the classical point of view of the fluctuations. Next, we will see how the curvature perturbations are conserved independently during reheating. Then, the origin of the primordial fluctuations will be explained. Afterwards, the field perturbation is converted into the curvature disturbance. Lastly, we will see how the statistics of it is related to the temperature difference of CMB.

4.1. Perturbed Scalar Field in Classical View Point

To start the whole discussion, it is crucial to know about the evolution of the field fluctuations first. Recall the inflaton action,

$$S = \int d\tau d^3x \sqrt{-g}\Big[\frac{1}{2}g^{\mu\nu}\partial_\mu\phi\partial_\nu\phi - V(\phi)\Big]. \tag{4.1.1}$$

Since the fluctuations are tiny compared to the mean value, we are allowed to do the perturbation theory with this action. Here, the perturbation term must be position-dependent since the CMB fluctuations have a different value at each point. Thus, we choose to perturb the field as

$$\phi(\tau,\vec{x}) = \bar{\phi}(\tau) + \frac{f(\tau,\vec{x})}{a(\tau)}, \tag{4.1.2}$$

where $\bar{\phi}(\tau)$ is the background field. We have redefined the field perturbations as $f(\tau,\vec{x}) = a(\tau)\delta\phi(\tau,\vec{x})$.

The field, which is the matter sector in the Einstein field equation, has been perturbed. For consistency, the geometry sector in the Einstein field equation must be perturbed as well. The perturbed FLRW metric tensor [31] can be generally written as

$$g_{\mu\nu} = a^2(\tau)\begin{pmatrix}1 & 0\\ 0 & -\mathbb{1}\end{pmatrix} + \delta g_{\mu\nu} = a^2(\tau)\begin{pmatrix}1+A & B_j\\ B_i & -(\mathbb{1}+C)\delta_{ij}+h_{ij}\end{pmatrix}. \tag{4.1.3}$$

Here, the metric is perturbed up to linear order of perturbation where A, C, B_i and h_{ij} are scalar, vector and tensor perturbations of the metric. In this case, all of these disturbances will be removed for the following reasons. First of all, h_{ij} does not contribute to the metric when keeping the perturbation up to second-order. This is because the lowest order coupling term between tensor and the field fluctuation existed in the action takes the form $h^{ij}\partial_i f\partial_j f$, which is already in third-order. This leaves

us with only the vector and scalar perturbations that can exist in the second-order action. Further from this, the vector perturbation does not contribute to this model. Since B_i is a vector that can only be sourced by a vector field via Einstein's field equation, the term will not evolve because there is no matter as a vector field in this model. The term thus dissipates due to the exponentially fast expansion of inflation. Finally, we are left with the scalar modes, A and C. A very convenient way to remove these variables is by changing the coordinate. We can choose the set of coordinates in which the scalar disturbance of the metric vanished and leaves only the scalar field fluctuation on a flat space. This is possible because there is only one scalar degree of freedom in this simplest model, which is introduced as the scalar field fluctuation above. Also, the theory of general relativity is invariant under this reparameterization because it is constructed by geometrical objects, e.g. tensors, which are independent of the choice of coordinates. Therefore, one can freely choose a variable to represent this degree of freedom in the action. This is called the *gauge fixing*. The choice of gauge made here will not affect the result of observable value whatsoever, it is just a preference of perspective. In this case, it's convenient to compute the field fluctuations in the action rather than the metric perturbations. Thus, the coordinates are chosen such that A and C are fixed to zero. This gauge is called the *spatially flat gauge* where the curvature has been fixed to zero.

Finally, the metric tensor reduces to the unperturbed FLRW metric tensor:

$$g_{\mu\nu} = a^2(\tau) \begin{pmatrix} 1 & 0 & 0 & 0 \\ 0 & -1 & 0 & 0 \\ 0 & 0 & -1 & 0 \\ 0 & 0 & 0 & -1 \end{pmatrix}. \tag{4.1.4}$$

Thus, one can consider only the scalar field perturbations without worrying about the dynamic coupling with the space-time geometry. Later, we will switch to another variable: curvature perturbation since it is the quantity that conserves during reheating. Lastly, the potential of the scalar field must be perturbed as well. Since the potential is a function of the field, one can perform the Taylor expansion as

$$V(\bar{\phi} + \frac{f}{a}) = V(\bar{\phi}) + V_{,\phi}\,\frac{f}{a} + V_{,\phi\phi}\left(\frac{f}{a}\right)^2 + \mathcal{O}(f^3). \tag{4.1.5}$$

By substituting the perturbed field and (4.1.5) into the action, the action yields

$$S = \int d\tau d^3x \Big[\frac{1}{2}a^2\Big[(\bar{\phi}' + \Big(\frac{f}{a}\Big)')^2 - \Big(\frac{\nabla f}{a}\Big)^2\Big] - a^4\Big[V(\bar{\phi}) + V_{,\phi}\,\frac{f}{a} + V_{,\phi\phi}\left(\frac{f}{a}\right)^2\Big]\Big]. \tag{4.1.6}$$

To study the dynamics of the perturbed field, the action will be extremized to derive the equation of motion. We can analyse each order of perturbations separately for convenience. It is commonly known that the zeroth-order of the action will return the background equation of motion. In this case, the zeroth-order gives the Klein-Gordon equation:

$$\bar{\phi}'' + 2\mathcal{H}\bar{\phi}' + a^2 V_{,\phi} = 0, \tag{4.1.7}$$

which is the same equation of motion in the previous section as expected. Next, the first-order action is

$$S^{(1)} = \int d\tau d^3x \Big[a\bar{\phi}' f' + a'\bar{\phi}' f - a^3 V_{,\phi}\, f\Big]. \tag{4.1.8}$$

The first term can be integrated by parts. By dropping the boundary term and simplifying the equation, the action is left as

$$S^{(1)} = \int d\tau d^3x \Big[\bar{\phi}'' + 2\mathcal{H}\bar{\phi}' + a^2 V_{,\phi}\Big] f. \tag{4.1.9}$$

From (4.1.7), one find that the first-order action is zero therefore the next order must be considered.

The second-order action is

$$S^{(2)} = \int d\tau d^3x \Big[f'^2 - \mathcal{H}(f^2)' - (\nabla f)^2 + (\mathcal{H}^2 - a^2 V_{,\phi\phi}) f^2 \Big]. \tag{4.1.10}$$

By integrating by parts the second term, the action becomes

$$S^{(2)} = \int d\tau d^3x \Big[f'^2 - (\nabla f)^2 + (\frac{a''}{a} - a^2 V_{,\phi\phi}) f^2 \Big]. \tag{4.1.11}$$

The slow-roll parameter, $\eta_V = \frac{M_{pl}^2 V_{,\phi\phi}}{V}$, is recalled. By applying the slow-roll potential approximation to the action, $\eta_V \ll 1$, one can argue that $\frac{a''}{a} = 2\mathcal{H}^2 \ll a^2 V_{,\phi\phi}$. Hence, the last term is reduced and the action is left as

$$S^{(2)} = \int d\tau d^3x \Big[f'^2 - (\nabla f)^2 + \frac{a''}{a} f^2 \Big]. \tag{4.1.12}$$

By extremizing the action, one gets the *Mukhanov-Sasaki equation*:

$$f'' - \nabla^2 f - \frac{a''}{a} f = 0, \tag{4.1.13}$$

which is the equation of motion of scalar field perturbation, $f(\tau, \vec{x})$. This equation tells us that the perturbation of inflaton field evolve like an oscillator with a time-dependent mass term. In Fourier space, each mode of perturbation satisfies the equation:

$$f_k'' + \Big(k^2 - \frac{a''}{a} \Big) f_k = 0. \tag{4.1.14}$$

4.2. The Curvature Perturbations

Previously, we consider the field fluctuations only by imposing the spatially flat gauge, which eliminates all of the metric perturbations. As mentioned at the beginning of this section, the essential quantity that delivered the primordial fluctuations out from inflation is the curvature perturbations. This is because it's conserved throughout the reheating to the time when the CMB emits. To show the conservation of the primordial fluctuations, it is convenient to change the choice of gauge before exiting the inflationary era. We will change to the coordinate in which the field fluctuation is set to zero and the fluctuation appears as a scalar metric perturbation, $\mathcal{R}$, also known as the curvature perturbation. This is the so-called *uniform density gauge* for the reason that the density fluctuations are fixed to zero. This subsection will discuss the conversion of the field fluctuation in the spatially flat gauge, $\delta\phi$, to the curvature fluctuation in the uniform density gauge. Consider the metric, the curvature fluctuations is defined as

$$ds^2 = a^2(\tau)[d\tau^2 - e^{2\mathcal{R}} \delta_{ij} dx^i dx^j] \approx a^2(\tau)[d\tau^2 - (1 + 2\mathcal{R}) \delta_{ij} dx^i dx^j]. \tag{4.2.1}$$

Here, the metric is perturbed to linear order. From this metric, we can compute the relation between the scalar field fluctuations and the curvature perturbations via the perturbed Einstein field equation. the result is

$$\mathcal{R}\Big|_{\text{uniform density gauge}} = -\frac{\mathcal{H}}{\bar{\phi}'} \delta\phi \Big|_{\text{spatially flat gauge}}. \tag{4.2.2}$$

The variable $\delta\phi$ is the scalar field fluctuation. For each Fourier mode of disturbances, the relation is

$$\mathcal{R}_k\Big|_{\text{uniform density gauge}} = -\frac{\mathcal{H}}{\bar{\phi}'} \delta\phi_k \Big|_{\text{spatially flat gauge}}. \tag{4.2.3}$$

From the relation, the disturbance of the curvature will be opposite to the field fluctuation due to the minus sign. The readers must keep in mind that this will not change the final results of the observable values whatsoever, it's just a choice to parameterize the single fluctuation degree of freedom. The disturbance here just simply can be visualized in several pictures. For example, this perturbation can also be described as uneven expansion. That is, the scale factor in the perturbed metric can be redefined as

$$\hat{a}(\tau, \vec{x}) = a(\tau)(1 + \mathcal{R}(\tau, \vec{x})). \tag{4.2.4}$$

Since the curvature perturbation is position-dependent, the redefined scale factor depends on the position. Thus, the fluctuations can also be thought of as the various amount of expansion among the points on x-space. To be more precise, if the curvature fluctuation is positive, space inflates more than average. If it's negative, space expands less than the mean. Just to mention another picture, the fluctuations here can also be considered as some point being behind/ahead of time (see Figure 4). This is because the unperturbed field in this gauge is a monotonic function of time, hence represents the evolution of inflation (one can think of it as a clock of inflation). That is, the curvature disturbance is equivalently shifting the evolution backward in time, which allows space to inflate more than average. The next topic will show that this quantity is conserved during reheating, this makes $\mathcal{R}$ an important quantity that links the fluctuations in inflation to the fluctuations of CMB temperature.

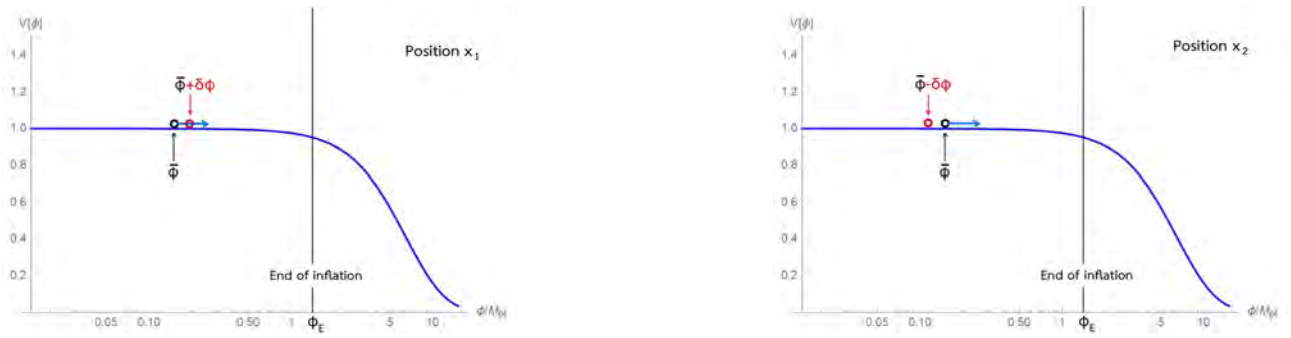

(a) Positive field fluctuation *(b) Negative field fluctuation*

Figure 4: An illustration of the fluctuation evolving on the inflaton potential on different position, x_1 and x_2. In (a), a positive $\delta\phi$ can be thought of as a part of space that evolving ahead of time. This corresponds to a negative value of R, or space inflates less than average because there is less time to inflate now. In picture (b) however, we say that the field is less than average on position x_2. The interpretation is the opposite: the evolution of the field here lacks behind the average value. Thus, space has more time to inflate and expands more than average. This corresponds to a positive R.

4.3. The Solution in de Sitter Space

From the equation of motion, the mass term in the equation is time-dependent. Thus, the behaviour of the field perturbations changes over time. To be more specific with the evolution, we are going to look into the evolution of the field fluctuations in detail. In this discussion, the perfect inflation background is assumed. Since the expansion in the perfect inflation is de Sitter expansion, the scale factor evolves as $a(\tau) \propto -\tau^{-1}$. The equation (4.1.14) becomes

$$f_k'' + \left(k^2 - \frac{2}{\tau^2}\right) f_k = 0. \tag{4.3.1}$$

From the equation (4.3.1), one can see that the behaviour of f_k depends on the value of k compared to τ^{-1}. To illustrate each behaviour separately, the *comoving Hubble radius* is introduced, which is a

sphere of radius defined as

$$\text{comoving Hubble Radius} \equiv (aH)^{-1} = \mathcal{H}^{-1}, \tag{4.3.2}$$

Inside the Hubble sphere, the rate of expansion is slower than the speed of light on the comoving coordinates. Thus, light can travel closer to the centre (measured in physical coordinates). If the light is outside the Hubble sphere, the expansion would have pushed the light away faster than the speed of it. Therefore, it will never reach the centre.

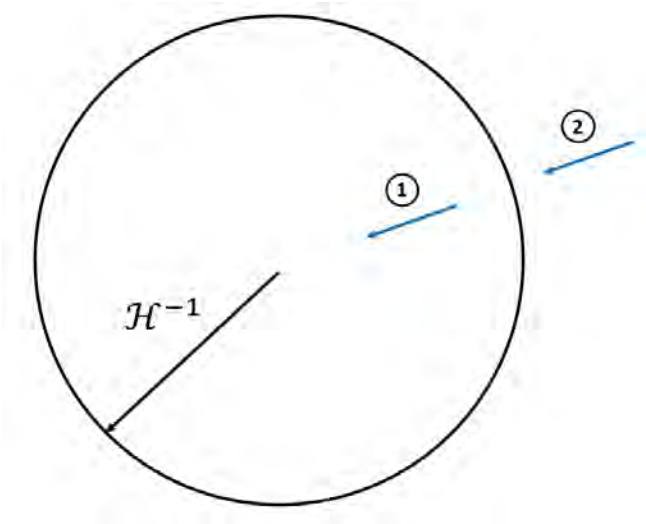

Figure 5: The comoving Hubble sphere is a spherical region with a Hubble radius of $\mathcal{H}^{-1}$. Position 1 shows a beam of light travel toward the centre located inside the sphere. There, the expansion is slower than the speed of light, which means light can move closer to the centre. In contrast, the light at point 2 outside the sphere will never reach the centre since the expansion pushes the light out faster than its speed.

For de Sitter expansion, the comoving Hubble radius takes the form of $\mathcal{H}^{-1} = -\tau$. Thus, the equation of motion takes the form:

$$f_k'' + (k^2 - 2\mathcal{H}^2) f_k = 0. \tag{4.3.3}$$

During inflation, the conformal time is increasing from a negative value ($\tau \in (-\infty, 0]$). Therefore, the comoving Hubble sphere is shrinking in inflation. In contrast, the wavelength of the perturbations, which related to k as $\lambda \sim k^{-1}$, remains constant on comoving coordinates [1]. The result is the comoving Hubble sphere will continue to shrink from very large to very small compared to k^{-1}. Therefore, the field perturbations change their behaviour over time. We are going to show the behaviour in the each following cases:

- **Super-horizon limit**: The comoving Hubble sphere continues to shrink down to the limit where the Hubble sphere is much smaller than the wavelength of the perturbation, $k \ll \mathcal{H}$. Here, the perturbations stop oscillating [32]. The equation is approximated to

$$f_k'' - \frac{2}{\tau^2} f_k = 0., \tag{4.3.4}$$

  By solving the equation exactly, the solution yields

$$f_k(\tau) = C_1 \tau^2 + C_2 \frac{1}{\tau}, \tag{4.3.5}$$

[1] One could think about it in the picture of physical coordinates as well. In this picture, the fluctuations are stretched out due to the expansion while the Hubble radius remains constant.

where C_1 and C_2 are some constants. To obtain the behaviour of the curvature disturbance, we transform the fluctuation f_k to the original form: $\delta\phi_k$. Then, we change the gauge to uniform density using the equation (4.2.3). The result is

$$\mathcal{R}_k = -\left(\frac{\mathcal{H}}{\bar{\phi}'}\right)(C_1\tau^3 + C_2) = -\frac{1}{M_{pl}\sqrt{2\epsilon}}(C_1\tau^3 + C_2).$$

From the previous discussion about inflation, the slow-roll parameter ϵ is hardly changed in inflation. Therefore, the multiplication term is approximately constant. Furthermore, the conformal time τ increases from negative value during inflation. One can argue that the second term, $C_1\tau^3$, decays. Thus, the only term left is the constant which implies that

$$\mathcal{R}_k \approx \text{constant (Super-horizon limit)}. \tag{4.3.6}$$

This tells us that the fluctuations at the super-horizon limit are fixed until inflation comes to an end. This is the mechanism that carried out the primordial perturbations nicely to the CMB. Notice that each mode of perturbations should proceed to this limit at a different time since the condition of this limit depends on k.

In fact, It has been shown in more generic way that $\mathcal{R}_k$ is always conserved in the super-horizon limit even if inflation has ended [33, 34]. The conservation law of it can be derived more generically from the cosmological perturbation theory. In this theory, the changing rate of $\mathcal{R}_k$ to the scale factor depends on the fraction of k over $\mathcal{H}$. This means $\mathcal{R}_k$ stop evolving when $k \ll \mathcal{H}$ in any period of the universe. Thus, one can rely on it to preserve the form of primordial fluctuations even if inflation has ended.

- **Sub-horizon limit**: If we consider the very early time of inflation, the conformal time approaches negative infinity. In that time, the comoving Hubble radius is much larger than the wavelength, $k \gg \mathcal{H}$. The equation of motion is reduced to

$$f_k'' + k^2 f_k = 0, \tag{4.3.7}$$

which is a simple harmonic oscillator with a frequency of k. This is because the oscillator's length scale is much smaller than the Hubble sphere to the point where expansion rate does not affect the oscillation anymore, corresponds to the absence of the term $\frac{a''}{a}$ in the equation of motion. By solving this boundary equation, the normalized solution is

$$f_k(\tau) = \frac{1}{\sqrt{2k}}e^{-ik\tau}. \tag{4.3.8}$$

This is the mode function for the so-called *Bunch-Davies vacuum* [35]. This mode function corresponds to the vacuum state of the inflaton fluctuations. To be more precise, there are actually two solutions for this equation, the positive frequency and the negative frequency. Here, only the positive frequency solution has been chosen. This is because we prefer the positive energy mode function for the ground state of the system.

Furthermore, one can solve the equation (4.3.1) and gets the exact solution:

$$f_k(\tau) = \alpha\frac{e^{-ik\tau}}{\sqrt{2k}}\left(1 - \frac{i}{k\tau}\right) + \beta\frac{e^{ik\tau}}{\sqrt{2k}}\left(1 + \frac{i}{k\tau}\right). \tag{4.3.9}$$

By using (4.3.8) to fix the coefficients $\alpha = 1$ and $\beta = 0$, the solution becomes

$$f_k(\tau) = \frac{e^{-ik\tau}}{\sqrt{2k}}\left(1 - \frac{i}{k\tau}\right). \tag{4.3.10}$$

This is the classical evolution of the scalar field fluctuations with mode k which corresponds to the vacuum state at each time. We will use this to calculate the quantum fluctuations around the ground state in the next subsection.

4.3.1. The Horizon Crossing

The horizon crossing refers to the point where $k = \mathcal{H}$. This is the point where the field fluctuations change their behaviour. To present this, it is convenient to change the variable in equation (4.3.3). By substituting the $\delta\phi_k$ back into the equation, we get

$$\delta\phi_k'' + 2\mathcal{H}\delta\phi_k' + k^2\delta\phi_k = 0. \tag{4.3.11}$$

The equation of motion is now a damped oscillator that critically damped at $k = \mathcal{H}$. Thus, the field perturbations stop oscillating at $k = \mathcal{H}$ and converge to a constant value exponentially. This emphasizes that each mode of fluctuations stopped oscillating at a different moment since the point of horizon crossing depends on k. Figure 6 illustrate the behaviour of the field fluctuations at different time.

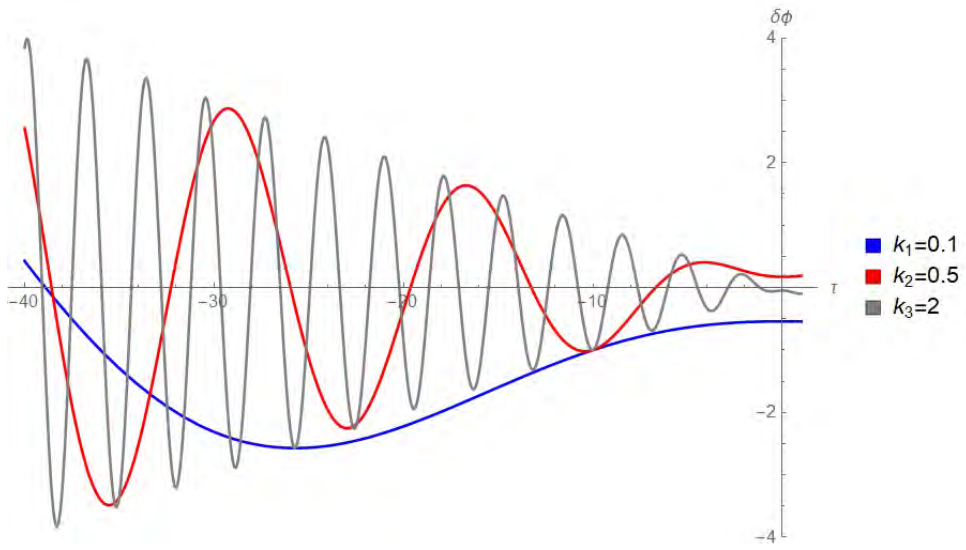

Figure 6: The behaviour of field fluctuations in de Sitter space at different time. Each mode stop oscillating at different time. For example, the fluctuation with $k = 0.1\ m^{-1}$ stops oscillating at $\tau = -10\ s$ but the fluctuation with $k = 0.5\ m^{-1}$ stops oscillating at $\tau = -2\ s$. (The exact amplitude of the field fluctuations remain unknown)

4.4. Quantum Fluctuations in de Sitter Space

The previous subsection has explained the evolution of the field fluctuations and labelled the point of fluctuations freezing, the horizon crossing. The next question would be "where do they come from?". As already mentioned, the quantum behaviour of the field is significant in inflation. In this case, the fluctuation is probabilistic due to quantum uncertainty [13–16]. Therefore, one should consider the statistics of the field rather than the deterministic classical picture. Intuitively, the rapid expansion stretched the quantum fluctuation of the field out. Then, these fluctuations curve the space-time creating the curvature perturbations. Thus, the quantum fluctuations of the field are the origin of the primordial fluctuations in inflation. As we mentioned before, the fluctuations are fully frozen at the super-horizon limit. These fluctuations should become classical at this limit. Thus, they can create the classical fluctuations seen in CMB. In this subsection, the statistics of the quantum fluctuations will be computed and show that it indeed becomes classical before inflation ends.

4.4.1. Harmonic Oscillator Quantization

Since the fluctuation in this context is probabilistic, the observable values are the statistical moments of the distribution. To compute the moments from the theory, the scalar field must be canonically quantized. Firstly, let us recall how to quantize a harmonic oscillator. In classical mechanics, the state of a system can be described by its position q and canonical momentum p. To quantize a classical system, the state variables q and p need to be promoted to operators that satisfy the canonical commutation relation:

$$[\hat{q}, \hat{p}] = i. \tag{4.4.1}$$

Here, we have set $\hbar \equiv 1$. Since each mode of the inflaton fluctuations behaves like a harmonic oscillator, a simple harmonic oscillator will be quantized as an example. In Hamiltonian formalism, the Hamiltonian determine the dynamics of the system. One finds that the energy of a classical system has a continuous range. In contrast, the energy of a quantum system is discrete. Thus, the Hamiltonian is promoted to an operator for a quantum system:

$$\hat{H} = \frac{1}{2}\hat{p}^2 + \frac{1}{2}\omega\hat{q}^2. \tag{4.4.2}$$

The variable ω is the angular frequency of the system. The energy of the system is now the eigenvalue of the Hamiltonian operator. For a classical system, the dynamics of the system can be determined by solving the equation of motion with the given initial conditions of q and p. These initial conditions correspond to the energy of the system. For a quantum system, we have spectra of energy levels rather than a continuous one. Thus, it is convenient to define the creation and annihilation operators that change the energy level of the system. These operators are defined to trade with the initial conditions of the system. Thus, we can conveniently raise/lower the energy rather than solving the equation of motion for every new initial condition. The creation and annihilation operators for simple harmonic oscillator are

$$\hat{a}^\dagger = \sqrt{\frac{\omega}{2}}\hat{q} - \frac{i}{\sqrt{2\omega}}\hat{p}, \tag{4.4.3}$$

$$\hat{a} = \sqrt{\frac{\omega}{2}}\hat{q} + \frac{i}{\sqrt{2\omega}}\hat{p}. \tag{4.4.4}$$

The creation operator, $\hat{a}^\dagger$, will raise the energy level. On another hand, the annihilation operator, $\hat{a}$, will lower the energy level. These operators can be inverted into

$$\hat{q} = \frac{1}{\sqrt{2\omega}}(\hat{a} + \hat{a}^\dagger), \tag{4.4.5}$$

$$\hat{p} = -i\sqrt{\frac{\omega}{2}}(\hat{a} - \hat{a}^\dagger). \tag{4.4.6}$$

By substituting these operators back into equation (4.4.1), we get the commutation relation:

$$[\hat{a}, \hat{a}^\dagger] = 1. \tag{4.4.7}$$

This is the quantization of a harmonic oscillator. Next, we will consider our field of interest, inflaton. As already shown, the perturbation of the field behaves like a oscillator. Thus, the quantization proceeds quite the same.

4.4.2. Field Quantization

A simple harmonic oscillator has been quantized. Next, we would like to do the same thing with the inflaton. The idea is the field $f(\tau, \vec{x})$ is an analogy with the variable q. We can define the canonical

conjugate field the same way we define the canonical momentum as

$$\pi \equiv \frac{\partial \mathcal{L}}{\partial f} = f', \tag{4.4.8}$$

which is an analogy with canonical momentum p, where $\mathcal{L}$ is the Lagrangian of the redefined fluctuations $f(\tau, \vec{x})$. The next step is to promote these fields to operators. Like before, the promoted field operators must satisfy a commutation relation, in this case, the equal time canonical commutation relation:

$$[\hat{f}(\tau, \vec{x}), \hat{\pi}(\tau, \vec{x}')] = i\delta^{(3)}(\vec{x} - \vec{x}'). \tag{4.4.9}$$

Notice that the promoted operators are in the Heisenberg picture, that is the state is time-independent but the operators may depend on time. Now we would like to quantize the energy level. Except now, we have an infinite possible mode of oscillators on each point of the field rather than a single oscillator[2]. This can be relatively simple if our field is a free field since the equation of motion of each mode does not couple with other modes and evolve independently. Since the derivative of potential term is neglected from the action due to the slow-roll condition, the fluctuations is a non-interacting field and its action indeed a free field action. Thus, it can be thought of a collection of independent harmonic oscillators. Therefore, the field operators can be expanded with creation and annihilation operators as

$$\hat{f}(\tau, \vec{x}) = \int \frac{d^3k}{(2\pi)^3} \left[f_k(\tau) e^{i\vec{k}\cdot\vec{x}} \hat{a}_{\vec{k}} + f_k^*(\tau) e^{-i\vec{k}\cdot\vec{x}} \hat{a}_{\vec{k}}^\dagger \right], \tag{4.4.10}$$

$$\hat{\pi}(\tau, \vec{x}) = \int \frac{d^3k}{(2\pi)^3} \left[f_k'(\tau) e^{i\vec{k}\cdot\vec{x}} \hat{a}_{\vec{k}} + (f_k'(\tau))^* e^{-i\vec{k}\cdot\vec{x}} \hat{a}_{\vec{k}}^\dagger \right]. \tag{4.4.11}$$

In Fourier space, the operators are

$$\hat{f}_{\vec{k}}(\tau) = f_k(\tau) \hat{a}_{\vec{k}} + f_k^*(\tau) \hat{a}^\dagger_{-\vec{k}}, \tag{4.4.12}$$

$$\hat{\pi}_{\vec{k}}(\tau) = f_k'(\tau) \hat{a}_{\vec{k}} + (f_k'(\tau))^* \hat{a}^\dagger_{-\vec{k}}. \tag{4.4.13}$$

The variable f_k is the normalized solution of the Mukhanov-Sasaki equation in Fourier space. The creation and annihilation operators are now labelled with a mode vector $\vec{k}$ associated with each mode of the oscillator. The creation and annihilation operators with different labelling will raise/lower the energy in different modes. As before, one gets the commutation relation of $\hat{a}_{\vec{k}}$ and $\hat{a}^\dagger_{\vec{k}}$:

$$[\hat{a}_{\vec{k}}, \hat{a}^\dagger_{\vec{k}'}] = (2\pi)^3 \delta^{(3)}(\vec{k} - \vec{k}') \tag{4.4.14}$$

by substituting the field operators into commutation relation of the field (4.4.9). This is called the *second quantization* for historical reason. Since the field fluctuates around the background value, it corresponds to the fluctuations around the ground state of the field $f(\tau, \vec{x})$. Thus, to compute the statistics of the generated fluctuations in inflation, one must calculate the fluctuations around the ground state of the system. The ground state is also known as *vacuum state* which is the state that satisfies the condition

$$\hat{a}_{\vec{k}} |0\rangle = 0, \qquad \forall \vec{k}. \tag{4.4.15}$$

This is the lower-bound state of the system. The statistical value of this fluctuation can be calculated as following:

- **Mean**: Mean of the fluctuations can be determined by calculating the expectation value of the

[2]This could be very hard to do so if one mode is coupled to the other. But, $f(\tau, \vec{x})$ is a free field in this case. Thus, each mode evolves independently.

field. Here, we are interested in the vacuum state:

$$\begin{aligned}\left\langle|\hat{f}|\right\rangle &= \langle 0|\,\hat{f}(\vec{x},\tau)\,|0\rangle \\ &= \int \frac{d^3k}{(2\pi)^3}\,\langle 0|\left[f_k(\tau)e^{i\vec{k}\cdot\vec{x}}\hat{a}_{\vec{k}} + f_k^*(\tau)e^{-i\vec{k}\cdot\vec{x}}\hat{a}_{\vec{k}}^\dagger\right]|0\rangle \\ &= \int \frac{d^3k}{(2\pi)^3} f_k^*(\tau)e^{-i\vec{k}\cdot\vec{x}}\,\langle 0|\,1\rangle \\ &= 0. \end{aligned} \tag{4.4.16}$$

Since we choose to calculate the fluctuation around the background value, the mean must indeed be zero because $f_k(\tau) = 0$ at the background value. This also benefits us when calculating the variance.

- **Variance**: Since we are calculating at the vacuum state, the mean of the fluctuation is absent. Therefore, the variance of the fluctuation is conveniently equal to the second moment of the fluctuations:

$$\begin{aligned}\left\langle|\hat{f}|^2\right\rangle &= \langle 0|\,\hat{f}^\dagger(\vec{x},\tau)\hat{f}(\vec{x},\tau)\,|0\rangle \\ &= \int \frac{d^3k}{(2\pi)^3}\int \frac{d^3k'}{(2\pi)^3}\,\langle 0|\left[f_k^*(\tau)e^{-i\vec{k}\cdot\vec{x}}\hat{a}_{\vec{k}}^\dagger + f_k(\tau)e^{i\vec{k}\cdot\vec{x}}\hat{a}_{\vec{k}}\right]\left[f_{k'}(\tau)e^{i\vec{k}'\cdot\vec{x}}\hat{a}_{\vec{k}'} + f_{k'}^*(\tau)e^{-i\vec{k}'\cdot\vec{x}}\hat{a}_{\vec{k}'}^\dagger\right]|0\rangle \\ &= \int \frac{d^3k}{(2\pi)^3}\int \frac{d^3k'}{(2\pi)^3}e^{i\vec{k}\cdot\vec{x}}e^{-i\vec{k}'\cdot\vec{x}}f_k(\tau)f_{k'}^*(\tau)\,\langle 0|\,[\hat{a}_{\vec{k}},\hat{a}_{\vec{k}'}^\dagger]\,|0\rangle \\ &= \int \frac{d^3k}{(2\pi)^3}\int \frac{d^3k'}{(2\pi)^3}e^{i\vec{k}\cdot\vec{x}}e^{-i\vec{k}'\cdot\vec{x}}(2\pi)^3\delta^{(3)}(\vec{k}-\vec{k}')|f_k(\tau)|^2 \\ &= \int \frac{d^3k}{(2\pi)^3}\int \frac{d^3k'}{(2\pi)^3}e^{i(\vec{k}-\vec{k}')\cdot\vec{x}}(2\pi)^3\delta^{(3)}(\vec{k}-\vec{k}')P_f(k,\tau). \end{aligned} \tag{4.4.17}$$

The integrand of this equation is the variance in Fourier space. The *power spectrum* of the field fluctuation, $P_f(k,\tau)$, is introduced as the variance's amplitude of each mode. From the expression, the power spectrum only depends on one of the two mode-vectors since the delta function would allow the variance to have some non-zero value only if $\vec{k} = \vec{k}'$. By substituting the solution (4.3.10), one gets

$$P_f(k,\tau) \equiv |f_{\vec{k}}(\tau)|^2 = \frac{1}{2k}\left(1 + \left(\frac{1}{k\tau}\right)^2\right). \tag{4.4.18}$$

As we are going to explain shortly, these eigenvalues that we computed quantum mechanically correspond to the statistical moments in the classical ensemble of the CMB fluctuation. This is because the quantum fluctuation here will become classical in the super-horizon limit, which is explained in the next subsection. Thus, this is where the dynamics of the field in inflation linked to the statistics of the CMB. The mean and variance here will be used to construct the probability density function (PDF) later in the subsection 4.6.

4.5. Primordial Fluctuation from Inflation

The previous discussion has told us about the important mechanism that carried the fluctuations out of inflation. The curvature fluctuations were conserved during the reheating and carried the primordial fluctuations from the field out. In this section, the quantum fluctuations of the field are converted into the classical curvature perturbations. Also, we will discuss the contributions given by primordial fluctuations to the CMB statistics.

4.5.1. Transition from Quantum to Classical

It has been shown that the fluctuations were produced quantum mechanically at the very early time of inflation. At the end, these will seed the CMB fluctuations which is classical. Thus, the field perturbations must become classical at some point before inflation has ended. Studies show that the field disturbances become classical at the super-horizon limit. To verify that, we would like to compute the commutation relation of the fields at that limit. If the field operators commute with its momentum conjugate, the fields are classical [36]. The field operators are

$$\hat{f}(\tau,\vec{x}) = \int \frac{d^3k}{(2\pi)^3}\big[f_k(\tau)e^{i\vec{k}\cdot\vec{x}}\hat{a}_{\vec{k}} + f_k^*(\tau)e^{-i\vec{k}\cdot\vec{x}}\hat{a}_{\vec{k}}^\dagger\big], \tag{4.5.1}$$

$$\hat{\pi}(\tau,\vec{x}) = \int \frac{d^3k}{(2\pi)^3}\big[f_k'(\tau)e^{i\vec{k}\cdot\vec{x}}\hat{a}_{\vec{k}} + (f_k'(\tau))^*e^{-i\vec{k}\cdot\vec{x}}\hat{a}_{\vec{k}}^\dagger\big]. \tag{4.5.2}$$

The time derivative of $f(k,\tau)$ is

$$f_{\vec{k}}'(\tau) = \frac{e^{-ik\tau}}{\sqrt{2k}}\Big(\frac{i}{k\tau^2}\Big) + (-ik)\frac{e^{-ik\tau}}{\sqrt{2k}}\Big(1-\frac{i}{k\tau}\Big). \tag{4.5.3}$$

One can compute both $f(k,\tau)$ and its time derivative in super-horizon limit and gets

$$f_{\vec{k}}(\tau)\Big|_{k\ll\mathcal{H}} = -\frac{e^{-ik\tau}}{\sqrt{2k^3}}\frac{i}{\tau},$$
$$f_{\vec{k}}'(\tau)\Big|_{k\ll\mathcal{H}} = \frac{e^{-ik\tau}}{\sqrt{2k^3}}\frac{i}{\tau^2}.$$

By substituting these functions into the quantum operators, one gets

$$\hat{f}(\vec{x},\tau)\Big|_{k\ll\mathcal{H}} = -\frac{i}{\sqrt{2}\tau}\int\frac{d^3k}{(2\pi)^3}\frac{1}{\sqrt{k^3}}[\hat{a}_{\vec{k}}e^{i(\vec{k}\cdot\vec{x}-k\tau)} + \hat{a}_{\vec{k}}^\dagger e^{-i(\vec{k}\cdot\vec{x}-k\tau)}]$$
$$\hat{\pi}(\vec{x},\tau)\Big|_{k\ll\mathcal{H}} = \frac{i}{\sqrt{2}\tau^2}\int\frac{d^3k}{(2\pi)^3}\frac{1}{\sqrt{k^3}}[\hat{a}_{\vec{k}}e^{i(\vec{k}\cdot\vec{x}-k\tau)} + \hat{a}_{\vec{k}}^\dagger e^{-i(\vec{k}\cdot\vec{x}-k\tau)}] = -\frac{1}{\tau}\hat{f}(\vec{x},\tau)\Big|_{k\ll\mathcal{H}}.$$

As expected, these operators commute at the super-horizon limit. This ensures that the quantum fluctuations become classical at that limit and create the classical curvature perturbations.

4.5.2. The Field Fluctuations at Super-horizon Limit

Now, we know that the field becomes classical at the super-horizon limit. Thus, before we transfer it into the curvature fluctuations, we would like to convert it back into the original field fluctuations $\delta\phi_k$ in de-Sitter space first. By substituting $f_{\vec{k}} = a\delta\phi_k$ back into the power spectrum of the field fluctuations (4.4.18), one gets

$$P_{\delta\phi}(k,\tau) \equiv a^{-2}P_f(k,\tau) = \frac{H^2}{2k\mathcal{H}^2}\Big(1+\Big(\frac{\mathcal{H}}{k}\Big)^2\Big). \tag{4.5.4}$$

We have assumed $\mathcal{H} = aH = -\tau^{-1}$ for de-Sitter expansion. By evaluating the power spectrum at the super-horizon limit, $k \ll \mathcal{H}$, one gets

$$P_{\delta\phi}(k)\Big|_{k\ll\mathcal{H}} = \frac{H^2}{2k^3}. \tag{4.5.5}$$

Interesting remarks about this are the following. First, the power spectrum is now time-independent. Thus, the fluctuations become constant like what we have discussed earlier. Second, the field fluctuations in this case are scale-invariant. To show this, we Fourier transform the power spectrum back

and receive the form:

$$\langle|\delta\phi|^2\rangle = \int d\ln k \Big(\frac{H}{2\pi}\Big)^2. \tag{4.5.6}$$

One can see that the Fourier component $\left(\frac{H}{2\pi}\right)^2$ does not depend on k, which implies that the fluctuations in de Sitter expansion are scale invariant [37] at the super-horizon limit. The visualization of this is the form of fluctuations look the same in every scale of CMB map.

However, this is not exactly the case in the actual result. Since the power spectrum above evaluates at the super-horizon limit of a specific k, thus it might hold a different value for each mode and hence depends on scale. This comes from the fact that the assumption made in subsection 4.3 that inflation undergoes de Sitter expansion until the limit of interest is a bit off from reality. In inflation, the expansion slows down and hence deviates from exponential expansion over time. Therefore, the fluctuation mode that reaches the super-horizon limit at a later time departs more from the scale-invariant form. As we're going to show later, the scale dependency of the fluctuation is actually determined by the slow-roll parameters, ϵ and η, which represent the departure from the exponential expansion. Nevertheless, let us continue to the curvature perturbation with the assumption and consider the scale dependency later.

4.5.3. The Curvature Perturbations at Super-horizon Limit

We have mentioned the relation between the field fluctuations and the curvature perturbations in the previous subsection. But now, we are interested in the statistics of the fluctuations. Thus, the variable $\mathcal{R}$ should be a statistical variable rather than a single deterministic value. One can square and average the equation (4.2.2) and gets the relation:

$$\langle|\mathcal{R}|^2\rangle = \Big(\frac{\mathcal{H}}{\bar{\phi}'}\Big)^2 \langle|\delta\phi|^2\rangle. \tag{4.5.7}$$

The variance of the curvature perturbations is the one that connects with the statistics of the CMB fluctuations. We are going to switch from the field fluctuations to the curvature perturbations via (4.5.7) at the super-horizon limit where the field fluctuations become classical. Let us recall the power spectrum of $\delta\phi$ at super-horizon limit (4.5.5). The power spectrum of the curvature perturbations at super-horizon limit takes the form:

$$P_{\mathcal{R}}(k)\Big|_{k\ll\mathcal{H}} = \Big(\frac{\mathcal{H}}{\bar{\phi}'}\Big)^2 \frac{H^2}{2k^3}\Big|_{k\ll\mathcal{H}}. \tag{4.5.8}$$

If we assume that inflation still undergoes the de Sitter expansion until the mode of interest reaches the super-horizon limit, the power spectrum can be expressed in the value evaluated at the horizon crossing:

$$P_{\mathcal{R}}(k)\Big|_{k\ll\mathcal{H}} = \Big(\frac{\mathcal{H}}{\bar{\phi}'}\Big)^2 \frac{H^2}{2k^3}\Big|_{k=\mathcal{H}}. \tag{4.5.9}$$

The power spectrum is now presented by the value at the horizon crossing to emphasize that the value of the power spectrum may vary among different modes. By exiting the horizon at different time, the modes with short wavelength might have reached the super-horizon limit when the expansion is not perfectly de Sitter expansion. This will make the power spectrum of short wavelength modes yield different value from this computed form.

If the slow-roll parameter, ϵ, is applied to the equation, one can find that the power spectrum of $\mathcal{R}$ can be determined by the shape of inflation slow-roll potential. By applying the definition of the slow-roll parameter in conformal time scale, $\epsilon \equiv \frac{\frac{1}{2}\bar{\phi}'}{M_{pl}^2\mathcal{H}^2}$, the equation becomes

$$P_{\mathcal{R}}(k)\Big|_{k\ll\mathcal{H}} = \frac{1}{2M_{pl}^2\epsilon}\frac{H^2}{2k^3}\Big|_{k=\mathcal{H}}. \tag{4.5.10}$$

Furthermore, we can assume the slow-roll potential. By substituting $\epsilon = \epsilon_V \equiv \frac{M_{pl}^2}{2}\left(\frac{V'}{V}\right)^2$ and $H^2 \approx \frac{V}{3M_{pl}^2}$, we have the form associated with the potential shape:

$$P_{\mathcal{R}}(k)\Big|_{k\ll\mathcal{H}} = \frac{1}{6M_{pl}^6 k^3}\frac{V^3}{V_{,\phi}^2}\Big|_{k=\mathcal{H}}. \tag{4.5.11}$$

This shows that the amplitude of fluctuations depends on the shape of the inflaton slow-roll potential. These are the statistics of the fluctuation that is carried out from inflation and appears on the CMB.

As mentioned, the form here is scale-invariant. But, we have already argued that this is the case only if the expansion does not slow down. Namely, the parameter ϵ stays constant at the horizon exit of every mode of perturbation. It is clearly not the case in real situation since the expansion slows down and ϵ varies with time. Hence, we expect the fluctuation to depend on scale by this effect. The next section will describe this scale dependency.

4.5.4. Scale-Dependent Power Spectrum

In the previous section, we obtained the scale-invariant power spectrum from the following assumption. Inflation undergoes the perfect de Sitter expansion until all of the modes reach the super-horizon limit. In reality, not all mode exits and reaches the super-horizon limit when the expansion is perfect de Sitter. This is because the slow-roll parameter ϵ will increase slowly during inflation and eventually equals 1 when inflation ends. This means that the expansion slowly deviates from perfect de Sitter over time. While the long modes (low momenta) reached the super-horizon limit when $\epsilon \approx 0$, the shorter modes (high momenta) would have reached when $\epsilon > 0$. From (4.5.10), we know that the power spectrum evaluates at the horizon crossing depends on the value of ϵ. Therefore, it will depend on scale. We will assume that the scale-dependence of the power spectrum takes the power-law form [38]:

$$P_{\mathcal{R}}(k) \propto k^{n_s - 4}. \tag{4.5.12}$$

The *scalar spectral index* n_s here represents the deviation from scale invariance of the power spectrum, which is defined as

$$n_s - 1 \equiv \frac{d\ln k^3 P_{\mathcal{R}}}{d\ln k}. \tag{4.5.13}$$

We are going to re-investigate the power spectrum evaluated at the horizon crossing, (4.5.10). One can clearly see that change of ϵ will affect the value of the power spectrum. By applying chain rule to the equation (4.5.13), we get

$$n_s - 1 = \frac{d\ln k^3 P_{\mathcal{R}}}{dN}\cdot\frac{dN}{d\ln k}. \tag{4.5.14}$$

By considering the first term, one can substitute equation (4.5.10) and the definition of slow-roll parameters ϵ and η into it and gets

$$\begin{aligned}\frac{d\ln k^3 P_{\mathcal{R}}}{dN} &= 2\frac{d\ln H}{dN} - \frac{d\ln\epsilon}{dN}\\ &= -2\epsilon - \eta.\end{aligned}$$

The second term can also be rearranged by evaluating it at the horizon crossing $k = \mathcal{H} = aH$,

$$\begin{aligned}\frac{dN}{d\ln k} &= \left[\frac{d\ln k}{dN}\right]^{-1}\\ &= \left[1 + \frac{d\ln H}{dN}\right]^{-1}\\ &= [1-\epsilon]^{-1} \approx 1 + \epsilon.\end{aligned}$$

By combining both terms via (4.5.14) and keeping the slow-roll parameter up to linear order, the expression becomes

$$n_s - 1 = -2\epsilon - \eta. \tag{4.5.15}$$

Therefore, the parameter n_s also represents the deviation from the perfect de Sitter expansion in slow-roll inflation corresponds with what we have discussed earlier. At the horizon crossing, the amount of deviation from de Sitter expansion determines how strong the power spectrum depends on scale. Furthermore, one can substitute back the potential slow-roll parameters and receives the relation between the spectral index and the inflaton's slow-roll potential:

$$n_s - 1 = -3M_{pl}^2\Big(\frac{V_{,\phi}}{V}\Big)^2 + 2M_{pl}^2\frac{V_{,\phi\phi}}{V}. \tag{4.5.16}$$

Recent observations from the Planck satellite [6] detected small deviation from the scale-invariance and measured $n_s = 0.9649 \pm 0.0042$ with 68% CL., statistically. The measurement also tells us how the slow-roll potential should look like via (4.5.16) (see Figure 3)

4.6. Statistics of the Primordial Fluctuations

We have described the primordial fluctuations. Now, one can ask about the statistics it gives to the CMB. It has been shown that the curvature perturbations are directly related to the temperature fluctuations of CMB through the *Sach-Wolfe approximation* on large-scale [39]. Thus, the statistics of the curvature perturbations are reflected directly in the temperature fluctuations. To study the contribution from the primordial fluctuations, it is convenient to consider the statistics of the curvature perturbations rather than the CMB temperature directly. Let us start with our simplest model and recall the action (4.1.12).

$$S^{(2)} = \int d\tau d^3x \Big[f'^2 - (\nabla f)^2 + \frac{a''}{a}f^2\Big]. \tag{4.6.1}$$

One can see that the action is quadratic since the inflaton's potential hardly changes in the slow-roll approximation. This implies Gaussian distributed field fluctuations which are reflected in the CMB fluctuations. To present the distribution, the probability density function (PDF) is constructed. In this case, the Gaussian PDF is fixed by mean and variance of the spread, which correspond to the computed eigenvalues (4.4.16) and (4.4.17). Since we have shown that the field perturbation will be converted into the curvature disturbance, which is the cause of CMB fluctuation, we choose to represent the distribution with a variable $\mathcal{R}_g$ as

$$\mathbf{G}(\mathcal{R}_g) = \frac{1}{\sigma\sqrt{2\pi}}e^{-\frac{\mathcal{R}_g^2}{2\sigma^2}}. \tag{4.6.2}$$

The variables $\mathcal{R}_g$ and σ are the curvature perturbation and the standard deviation of the distribution. Shortly, we will argue that the distribution can be something else other than normal. Thus, the Gaussian distributed variable, $\mathcal{R}_g$, is sub-scripted by g for distinction. In the context of $\mathcal{R}_g$, it is mean is set to zero since the variable fluctuates around the background value as mentioned in (4.4.16). The variance, which is the squared standard deviation: σ^2, corresponds to the power spectrum (4.5.10). At this point, the PDF is fully constructed and the higher-order statistical moments can be computed by

$$\langle \mathcal{R}_g^n \rangle = \int d\mathcal{R}_g\, \mathcal{R}_g^n \mathbf{G}(\mathcal{R}_g). \tag{4.6.3}$$

By calculating the moments above, one finds that the odd-order moments can be written as products of the mean. Thus, all of the odd-order statistical moments vanish since the mean is zero. This corresponds to one of the important properties of this PDF: the distribution curve is symmetric about the

mean value (no skewness). Furthermore, all of the even-order moments can be represented with products of the variance, which implies that the statistics of the Gaussian variable is completely described by the variance only. So far, the prediction of Gaussian fluctuation agreed with the observations[5–7]. So, a well-probed power spectrum could be the end of the story here.

However, the measurements have uncertainty which can hide non-Gaussian signatures from us, so one can expect that the distribution is not exactly Gaussian. This is motivated by the fact that there are possible features beyond the simplest model that can produce primordial non-Gaussianity. For example, there might be additional fields other than inflaton active during inflation, the multi-field scenario. Those fields might induce non-Gaussianity to the statistics even if the density of those fields are minorities compared to inflaton and do not affect the dynamics of inflation. This is because, when perturbing the action, the derivative of the potential with respect to those fields might be significant and cannot be neglected. Hence, the action may be non-quadratic in this case. Therefore, we might detect the deviations from the Gaussian distribution produced by primordial fluctuations by increasing the accuracy and learn more about the physics of inflation that causes the departure from the normal distribution.

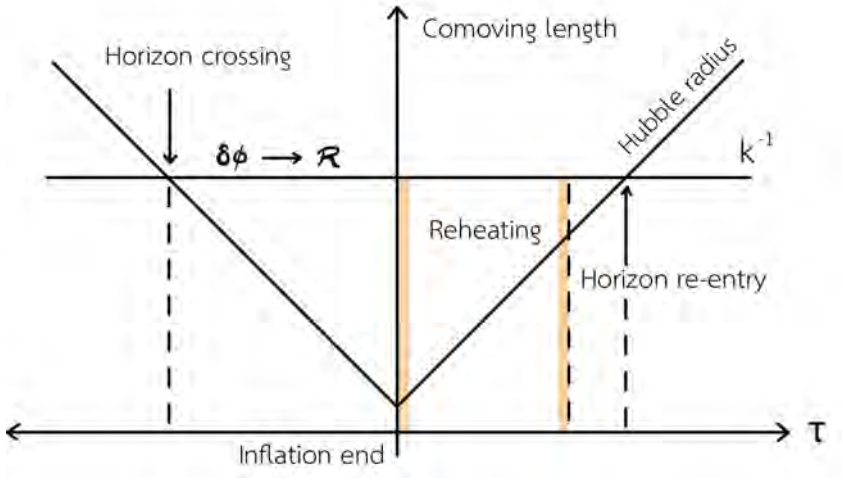

Figure 7: A full picture of the primordial fluctuations transportation process summarizes all of the procedures described in this section.

4.7. Overview of the Process

To summarize this section, the behaviour of the scalar field perturbations are described as an oscillator. The fluctuations of the scalar field perturbations are arisen from the quantum uncertainty and are stretched out by the expansion in inflation. The crucial point here is the fluctuations stopped oscillating at the horizon crossing and are frozen at the super-horizon limit. This hence delivered the primordial fluctuations across the period of unknown physics. After the perturbations crossed back into the horizon, the fluctuations evolved determinedly and then created the CMB temperature fluctuations. This has allowed us to study the physics of the early universe via the statistics of the CMB. Until now, the CMB fluctuations are found to be Gaussian distributed agreed with our simplest model. But recently, the primordial non-Gaussianity is the topic in the spotlight. The detection of it can reveal some new information about inflation. Further discussions will focus on the primordial non-Gaussianity and its implication.

5. Non-Gaussian Statistics of the Primordial Fluctuations

As mentioned in the last section, the distribution of the field is related to its action. Also, the features beyond the simplest model are expected. Thus, we can reveal some more complicated model of inflation by studying the statistics of the curvature perturbations in details. Namely, if one knows the exact probability density function (PDF) of the perturbations, one can derive the true action from it. This will give us more details about the physics in inflation, for instance, the structure of the interactions. From the previous section, we know that the simplest model corresponds to the normally distributed field. Therefore, we are interested in the deviation from it. Presently, the surveys [7] already told us that this deviation is small. Thus, we can write down the exact variable of curvature perturbation, $\mathcal{R}$, as a small perturbation to the Gaussian variable, $\mathcal{R}_g$ [19, 20]:

$$\mathcal{R} = \mathcal{R}_g + f(\mathcal{R}_g). \tag{5.0.1}$$

The arbitrary function $f(\mathcal{R}_g)$ is the perturbation to the Gaussian distribution. If the fluctuation is produced by the simplest model, the exact variable would be equal to the normally distributed variable, $\mathcal{R}_g$, in an absence of $f(\mathcal{R}_g)$. Thus, the perturbation function here is taking account of the additional features that produce non-Gaussianity to the distribution. The task here is to constrain this function from the observation and interprets the result to some implications about inflation. For instance, one can take the power-law ansatz and measure its amplitude from the survey to justify the existence of power-law interaction terms in the action.

We can observe the difference between the normally and exactly distributed variable by measuring the statistical moments of the true distribution and compare them to the Gaussian ones. From the last section, the normal distribution has zero odd-order moments and the even-orders determined by its variance. For the true statistics, we suppose that $\mathcal{R}$ obeys the true PDF, $\mathbf{P}(\mathcal{R})$. Its nth-order moment thus can be computed from

$$\left\langle \mathcal{R}^n \right\rangle = \int d\mathcal{R}\, \mathcal{R}^n \mathbf{P}(\mathcal{R}). \tag{5.0.2}$$

Shortly, we will see that the moments here serve as corrections to the Gaussian PDF. To mention intuitively how this is the case, we show the following example: we have mentioned that all of the odd-order moments in normal distribution vanish. However, for the exact PDF, one might notice that they do not have to vanish anymore. This is because the deviation, $f(\mathcal{R}_g)$, could have ruined the symmetry of the curve (see Figure 8) so that the moments cannot be determined by the mean as before. Thus, one of the straightforward non-Gaussianity signatures that can be detected is the non-vanishing odd-order moments. Therefore, they could tell us how the correct PDF should look like. To see how it is mathematically, we will discuss a way to evaluate $\mathbf{P}(\mathcal{R})$.

As mentioned at first, the task here is to find a way to describe the true PDF from which we can describe the action of the field. Since the departure from the normal distribution is small, the true PDF can be written as the Taylor series around the Gaussian PDF:

$$\mathbf{P}(\mathcal{R}) = \sum_{n=0}^{\infty} a_n \frac{d^n \mathbf{G}(\mathcal{R}_g)}{d\mathcal{R}_g^n}, \tag{5.0.3}$$

where a_n is the nth-order Taylor coefficient. After evaluating all of the derivatives, the series are

chosen to be rearranged as[3]

$$\mathbf{P}(\mathcal{R}) = \mathbf{G}(\mathcal{R}_g)\Big[1 + \sum_{n=1}^{\infty} c_n He_n(\mathcal{R}_g/\sigma)\Big] \tag{5.0.4}$$

for convenience. The special function He_n is the nth-order *Hermite polynomial* and c_n is the corresponding coefficient in front of it. The goal here is to determine c_n, which serves as a correction for the PDF. In this arrangement, they are conveniently determined by using the orthogonality with respect to Gaussian measure of $He_n(\mathcal{R})$. From there, one finds that those coefficients are combinations of the statistical moments. Thus, the goal here is to compute those moments to be the corrections as intuitively mentioned. In order to do so, we need the ansatz of $f(\mathcal{R}_g)$ first. One of the form was proposed by Eiichiro Komatsu and David N. Spergel [18] which is written as power series expansion:

$$\mathcal{R}(\vec{x}) = \mathcal{R}_g(\vec{x}) + \frac{3}{5} f_{NL}(\mathcal{R}_g^2(\vec{x}) - \langle \mathcal{R}_g^2(\vec{x}) \rangle) + \frac{9}{25} g_{NL} \mathcal{R}_g^3(\vec{x}) + \dots \ . \tag{5.0.5}$$

The parameters f_{NL} and g_{NL} are the non-linear parameters. The factors $\frac{3}{5}$ and $\frac{9}{25}$ are conventional for historical reasons. The form here is written such that the mean of it is zero as mentioned earlier. This is often called the *local-form* non-Gaussianity since the non-linear coupling of $\mathcal{R}_g$ and other terms are on the same point on x-space. Thus, this form will capture the non-Gaussianity that has been produced locally on x-space. As mentioned before, one can choose different ansatzes to capture other features. For example, the nonlinear term can be the sine function of $\mathcal{R}_g$, which we are going to discuss later. Also, the ansatz can be the gradient squared or laplacian of $\mathcal{R}_g$, $(\vec{\nabla}\mathcal{R}_g)^2$ or $\nabla^2\mathcal{R}_g$. In any case, the moments can now be computed. To begin the computation, the n-point function will be expanded just to the first-order of the parameter f_{NL}. This is because the observations [7] have already constrained the fluctuations to be tiny. Thus, the higher-order terms of $\mathcal{R}_g$, the term with g_{NL} for example, are neglected. The main goal of this section is to compute f_{NL}. Namely, we will compute the two- and three-point correlation functions and see how they related to the parameter. It will be later shown in this section that the three-point function is directly proportional to f_{NL}. Thus, the parameter is needed for the corrections. Moreover, it is also the measure of local non-Gaussianity as proposed in the form.

Broadly speaking, the correlation functions in this context are quite similar to the scattering amplitude in particle physics. As we are going to show shortly, the computation of the three-point function will give us the parameter f_{NL}, which is responsible for the additional interaction in the theory. Thus, the computation roughly gives the amplitude of the interaction, similar to the scattering amplitude. In this section, we will derive the formula that is used to compute f_{NL} from the observable value.

To give some ideas of what we expect f_{NL} to be, we are going to start with a broad discussion about its theoretical constrain. Since the statistics of $\mathcal{R}$ deviated from Gaussian just a bit, the non-linear terms must be tiny, compared to the first term. That is, the parameter must be much smaller than the order of $(\mathcal{R}_g)^{-1}$. However, the perturbations are found to be in the order of 10^{-5}. Thus, the parameter still has a wide range of value. For instance, $f_{NL} \sim 10^3$ is still theoretically allowed. From the most recent observation [7], the measured value of it is in the order 10^0, which is still tiny compared to the theoretical upper-bound. Hence, one can expect a noticeable magnitude of f_{NL} measured from the future observation. Before the computations, the expanded variable are Fourier transformed to

$$\mathcal{R}(\vec{k}) = \mathcal{R}_g(\vec{k}) + \frac{3}{5} f_{NL} \int \frac{d^3k'}{(2\pi)^3} \Big[\mathcal{R}_g(\vec{k}')\mathcal{R}_g(\vec{k} - \vec{k}') - \langle \mathcal{R}_g(\vec{k}')\mathcal{R}_g(\vec{k} - \vec{k}') \rangle \Big] + \dots \ . \tag{5.0.6}$$

As mentioned earlier, we will be focusing on the parameter f_{NL} only. Thus, the perturbation with be

[3] In general, any power series can be rearranged to series of Hermite polynomial.

kept just to the second-order. Next, we would like to compute the two-point and three-point functions and see how they related to the parameter f_{NL}. First, the two-point function, or the second moment, is

$$\langle \mathcal{R}(\vec{k})\mathcal{R}(\vec{k}')\rangle = \langle \mathcal{R}_g(\vec{k})\mathcal{R}_g(\vec{k}')\rangle + \frac{3}{5} f_{NL} \cdot \mathcal{O}(\mathcal{R}^3). \tag{5.0.7}$$

The second term is the three-point of the Gaussian variable, which is zero in this case. Thus, the second term vanishes along with the higher-order terms, which are sufficiently small. In conclusion, the two-point function of the non-Gaussian variable approximately equals the two-point function of the Gaussian variable. From the last section, this function of normally distributed fluctuation in Fourier space is written as

$$\langle \mathcal{R}_g(\vec{k})\mathcal{R}_g(\vec{k}')\rangle = (2\pi)^3 \delta^{(3)}(\vec{k}+\vec{k}') P_{\mathcal{R}}(|\vec{k}|), \tag{5.0.8}$$

where $P_{\mathcal{R}}(|\vec{k}|)$ is the power spectrum of the curvature fluctuations, the same one as in the last section. This is also the data that we can measure from the CMB temperature map. Generally speaking, the two-point correlation function is measured by counting pairs of the equal temperature points separated by the given length, k^{-1} (see Figure 13). The presence of the delta function indicates that the total k-vector of the two-point function must be a null vector (infinite length scale). This implies that the two-point function remains the same by the change of position (a homogeneous function on x-space).

The next step is to calculate the three-point of the non-Gaussian variable. Intuitively, the first term should be the three-point function of $\mathcal{R}_g$ which equals zero. Thus, the main contribution comes from the next term, the four-point function of $\mathcal{R}_g$. Furthermore, The four-point function of the Gaussian distributed variables is up to the square of the variance. This is because the four-point function of Gaussian variables can be expanded into a series of two-point functions via *Wick's theorem*. Thus, the three-point function is proportional to the variance of $\mathcal{R}_g$ squared. To compute the result exactly, let us first write the function with (5.0.6) as

$$\begin{aligned}\langle \mathcal{R}(\vec{k_1})\mathcal{R}(\vec{k_2})\mathcal{R}(\vec{k_3})\rangle =& \langle \mathcal{R}_g(\vec{k_1})\mathcal{R}_g(\vec{k_2})\mathcal{R}_g(\vec{k_3})\rangle \\ &+ \frac{3}{5} f_{NL}\Bigg[\Big\langle \int \frac{d^3k_1'}{(2\pi)^3}\Big[\mathcal{R}_g(\vec{k_1}')\mathcal{R}_g(\vec{k_1}-\vec{k_1}') - \langle \mathcal{R}_g(\vec{k_1}')\mathcal{R}_g(\vec{k_1}-\vec{k_1}')\rangle\Big]\mathcal{R}_g(\vec{k_2})\mathcal{R}_g(\vec{k_3})\Big\rangle \\ &+ \text{perm.}\Bigg].\end{aligned}$$

The first term vanishes since $\mathcal{R}_g(\vec{k})$'s are Gaussian variables. Therefore, the remaining terms are

$$\langle \mathcal{R}(\vec{k_1})\mathcal{R}(\vec{k_2})\mathcal{R}(\vec{k_3})\rangle = \frac{3}{5} f_{NL}\Bigg[\Big\langle \int \frac{d^3k_1'}{(2\pi)^3}\Big[\mathcal{R}_g(\vec{k_1}')\mathcal{R}_g(\vec{k_1}-\vec{k_1}') - \langle \mathcal{R}_g(\vec{k_1}')\mathcal{R}_g(\vec{k_1}-\vec{k_1}')\rangle\Big]\mathcal{R}_g(\vec{k_2})\mathcal{R}_g(\vec{k_3})\Big\rangle + \text{perm.}\Bigg]. \tag{5.0.9}$$

For convenience, only one of the permuted terms inside the square brackets is considered since the rest will yield the same with permuted k-vectors. An individual term can be simplified as

$$\begin{aligned}(\dots) &= \Big\langle \int \frac{d^3k_1'}{(2\pi)^3}\Big[\mathcal{R}_g(\vec{k_1}')\mathcal{R}_g(\vec{k_1}-\vec{k_1}') - \langle \mathcal{R}_g(\vec{k_1}')\mathcal{R}_g(\vec{k_1}-\vec{k_1}')\rangle\Big]\mathcal{R}_g(\vec{k_2})\mathcal{R}_g(\vec{k_3})\Big\rangle \\ &= \int \frac{d^3k_1'}{(2\pi)^3}\langle \mathcal{R}_g(\vec{k_1}')\mathcal{R}_g(\vec{k_1}-\vec{k_1}')\mathcal{R}_g(\vec{k_2})\mathcal{R}_g(\vec{k_3})\rangle - \int \frac{d^3k_1'}{(2\pi)^3}\langle \mathcal{R}_g(\vec{k_1}')\mathcal{R}_g(\vec{k_1}-\vec{k_1}')\rangle\langle \mathcal{R}_g(\vec{k_2})\mathcal{R}_g(\vec{k_3})\rangle.\end{aligned}$$

From Wick's theorem, the four-point function can be expanded as

$$\langle f_1 f_2 f_3 f_4\rangle = \langle f_1 f_2\rangle\langle f_3 f_4\rangle + \langle f_1 f_3\rangle\langle f_2 f_4\rangle + \langle f_1 f_4\rangle\langle f_2 f_3\rangle, \tag{5.0.10}$$

where f_i's are Gaussian variables. Thus, one can expand the four-point function as such and gets

$$\begin{aligned}(\dots) &= \int \frac{d^3k_1'}{(2\pi)^3}\Big[\langle\mathcal{R}_g(\vec{k_1}')\mathcal{R}_g(\vec{k_1}-\vec{k_1}')\rangle\langle\mathcal{R}_g(\vec{k_2})\mathcal{R}_g(\vec{k_3})\rangle + \langle\mathcal{R}_g(\vec{k_1}')\mathcal{R}_g(\vec{k_2})\rangle\langle\mathcal{R}_g(\vec{k_1}-\vec{k_1}')\mathcal{R}_g(\vec{k_3})\rangle \\ &\quad + \langle\mathcal{R}_g(\vec{k_1}')\mathcal{R}_g(\vec{k_3})\rangle\langle\mathcal{R}_g(\vec{k_1}-\vec{k_1}')\mathcal{R}_g(\vec{k_2})\rangle\Big] - \int \frac{d^3k_1'}{(2\pi)^3}\langle\mathcal{R}_g(\vec{k_1}')\mathcal{R}_g(\vec{k_1}-\vec{k_1}')\rangle\langle\mathcal{R}_g(\vec{k_2})\mathcal{R}_g(\vec{k_3})\rangle \\ &= \int \frac{d^3k_1'}{(2\pi)^3}\Big[\langle\mathcal{R}_g(\vec{k_1}')\mathcal{R}_g(\vec{k_2})\rangle\langle\mathcal{R}_g(\vec{k_1}-\vec{k_1}')\mathcal{R}_g(\vec{k_3})\rangle + \langle\mathcal{R}_g(\vec{k_1}')\mathcal{R}_g(\vec{k_3})\rangle\langle\mathcal{R}_g(\vec{k_1}-\vec{k_1}')\mathcal{R}_g(\vec{k_2})\rangle\Big].\end{aligned}$$

From (5.0.8), the two-point functions are written in the form of the power spectra:

$$\begin{aligned}(\dots) =&(2\pi)^3\int d^3k_1'\Big[\delta^{(3)}(\vec{k_1}'+\vec{k_2})\delta^{(3)}(\vec{k_1}-\vec{k_1}'+\vec{k_3})P_{\mathcal{R}}(|\vec{k_2}|)P_{\mathcal{R}}(|\vec{k_3}|) \\ &+\delta^{(3)}(\vec{k_1}'+\vec{k_3})\delta^{(3)}(\vec{k_1}-\vec{k_1}'+\vec{k_2})P_{\mathcal{R}}(|\vec{k_2}|)P_{\mathcal{R}}(|\vec{k_3}|)\Big] \\ =&(2\pi)^3\Big[2\delta^{(3)}(\vec{k_1}+\vec{k_2}+\vec{k_3})P_{\mathcal{R}}(|\vec{k_2}|)P_{\mathcal{R}}(|\vec{k_3}|)\Big].\end{aligned}$$

By substituting this back into (5.0.9), one gets the three point function with the parameter f_{NL}:

$$\langle\mathcal{R}(\vec{k_1})\mathcal{R}(\vec{k_2})\mathcal{R}(\vec{k_3})\rangle = \frac{6}{5}f_{NL}(2\pi)^3\delta^{(3)}(\vec{k_1}+\vec{k_2}+\vec{k_3})\Big[P_{\mathcal{R}}(|\vec{k_2}|)P_{\mathcal{R}}(|\vec{k_3}|)+\text{perm.}\Big]. \tag{5.0.11}$$

Similar to the two-point function, the presence of delta function implies that the three-point function is a homogeneous function on x-space. One can define the bispectrum from the function as

$$\langle\mathcal{R}(\vec{k_1})\mathcal{R}(\vec{k_2})\mathcal{R}(\vec{k_3})\rangle = (2\pi)^3\delta^{(3)}(\vec{k_1}+\vec{k_2}+\vec{k_3})B_{\mathcal{R}}(|\vec{k_1}|,|\vec{k_2}|,|\vec{k_3}|). \tag{5.0.12}$$

The bispectrum is defined as the amplitude of the three-point function in Fourier space, similar to the power spectrum for the two-point function. From (5.0.11) and (5.0.12), the nonlinear parameter f_{NL} is determined via the formula

$$\frac{6}{5}f_{NL} = \frac{B_{\mathcal{R}}(|\vec{k_1}|,|\vec{k_2}|,|\vec{k_3}|)}{P_{\mathcal{R}}(|\vec{k_1}|)P_{\mathcal{R}}(|\vec{k_2}|)+P_{\mathcal{R}}(|\vec{k_2}|)P_{\mathcal{R}}(|\vec{k_3}|)+P_{\mathcal{R}}(|\vec{k_3}|)P_{\mathcal{R}}(|\vec{k_1}|)}. \tag{5.0.13}$$

The bispectrum and the power spectrum in this equation can be measured from the observations and

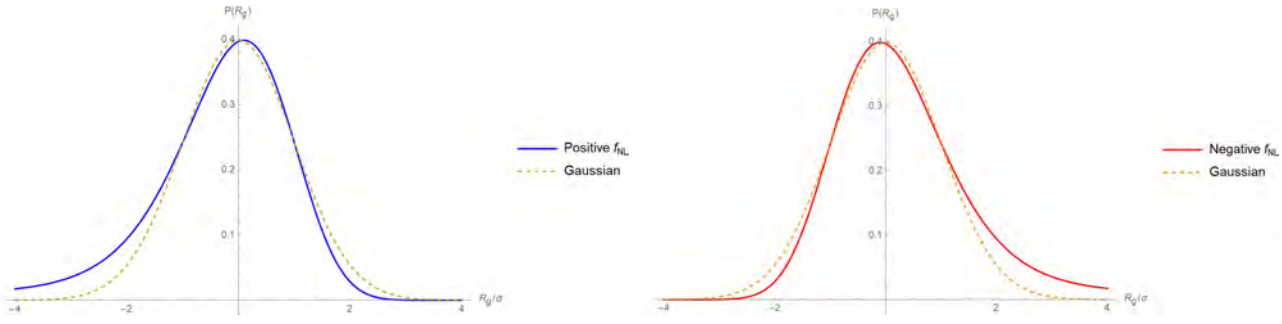

(a) Positive value of f_{NL} *(b) Negative value of f_{NL}*

Figure 8: The plot of probability density function when perturbed with parameter f_{NL}. In this case, the curves are (a) negatively skewed when f_{NL} is positive, and (b) positively skewed when f_{NL} is negative.

then used to determine the value of the nonlinear parameter f_{NL}. To visualize the effect, the non-zero parameter f_{NL} will add the skewness to the PDF. Namely, the probability curve will be tilted as shown in Figure 8. The observation [7] has measured the parameter as $f_{NL} = -0.9 \pm 5.1$, where the error bar covers up to 68% CL. of the statistics.

This is just one form of f_{NL} obtained from the power series ansatz we take for the perturbation function, $f(\mathcal{R}_g)$. There are also other interesting cases of it that correspond to other forms of the function. A different f_{NL} indicates different implications to our inflationary model. For sake of clear observation, we would like to fix the parameter at the peak value of the bispectrum. This is because the observed signal will be the most notable, thus the most convenient to probe. From the definition, it is labelled by the mode vectors, $\vec{k_1}$, $\vec{k_2}$ and $\vec{k_3}$. The constraint from the homogeneity requires these mode vectors to sum to null vector, thus they form a triangle shape. A different case of non-Gaussianity has its shape of bispectrum at which its value peaks. In this case, the bispectrum peaks at the so-called *squeezed limit* where the triangle of mode-vector effectively gets squeezed to a line. In the next section, we will discuss the importance of the shape.

6. The Squeezed Bispectrum

One of the well-known results first computed by Juan Maldacena [40] is the *squeezed bispectrum*. This bispectrum consists of two long k-vectors and one short k-vector (in other words, one long-wavelength mode and two short-wavelength modes), $k_1 \approx k_2 \gg k_3 \longrightarrow 0$. This kind of bispectrum serves as an attempt to rule out all single-field model of inflation. As we will see shortly, the single-field models predicted that the squeezed bispectrum should be tiny compared to the power spectrum squared. Thus, the detection of this bispectrum could conveniently rule out all single-field models despite their details. In this section, the squeezed bispectrum will be computed in a classical picture.

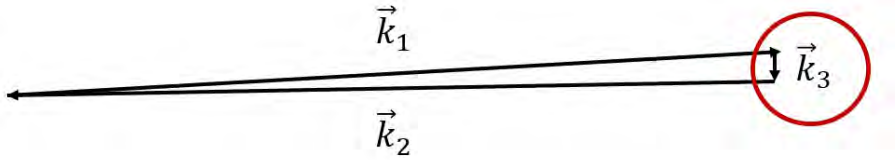

Figure 9: The triangle of the bispectrum's mode vectors in the squeezed limit, $k_1 \approx k_2 \gg k_3 \longrightarrow 0$. Here, the triangle has effectively degenerated to a line. This is because the norm of $\vec{k}_3$ is approaching zero as shown in the red circle.

Before going into the computation, let us discuss briefly the emergence of the three-point correlation function in the single-field scenario. As already mentioned, the squeezed bispectrum consists of one long-wavelength mode and two short-wavelength modes. At one time during inflation, the long-wavelength mode reached the super-horizon limit and became frozen as discussed in subsection 4.3. Thus, it becomes a constant disturbance of space-time. Meanwhile, the two short modes would be deeply in the horizon and still evolving on the background space-time perturbed by the frozen mode. Thus, those fluctuations will be affected by the long mode disturbance, which is now a part of the background. The consequence is these short and long modes will be correlated to each other via these processes. Hence, the three-point function of these modes emerged.

The goal here is to detect this non-Gaussianity in the observations. Since the power spectrum is nearly scale-invariant (see subsection 4.5.4), one can see from (5.0.11) and (4.5.12) that the bispectrum peaks when the magnitude of $\vec{k}$ approaching zero. Thus, the squeezed limit is considered because one of the k-vectors is approaching zero in this limit. Therefore, it will make the squeezed bispectrum the most noticeable signal of all in this case.

The first computation [40] was done in slow-roll inflation by using the Quantum Field Theory approach. Then, the result is extended by Creminelli and Zaldarriaga [22]. They have shown that the result is true for all single-field model, regardless of slow-roll condition. The method is nicely reviewed and enhanced by Jonathan Ganc and Eiichiro Komatsu [21]. The following computation is similar to Creminelli and Zaldarriaga's computation and to what Ganc and Komatsu have reviewed in their paper.

Since the long mode perturbation has already exited the horizon and became constant, the three-point function is written as

$$\left\langle \mathcal{R}_S(\vec{k_1})\mathcal{R}_S(\vec{k_2})\mathcal{R}_L(\vec{k_3})\right\rangle = \left\langle \left\langle \mathcal{R}_S(\vec{k_1})\mathcal{R}_S(\vec{k_2})\right\rangle_L \mathcal{R}_L(\vec{k_3})\right\rangle. \tag{6.0.1}$$

The expression $\left\langle \mathcal{R}_S(\vec{k_1})\mathcal{R}_S(\vec{k_2})\right\rangle_L$ is the two-point function of two short modes that are influenced by

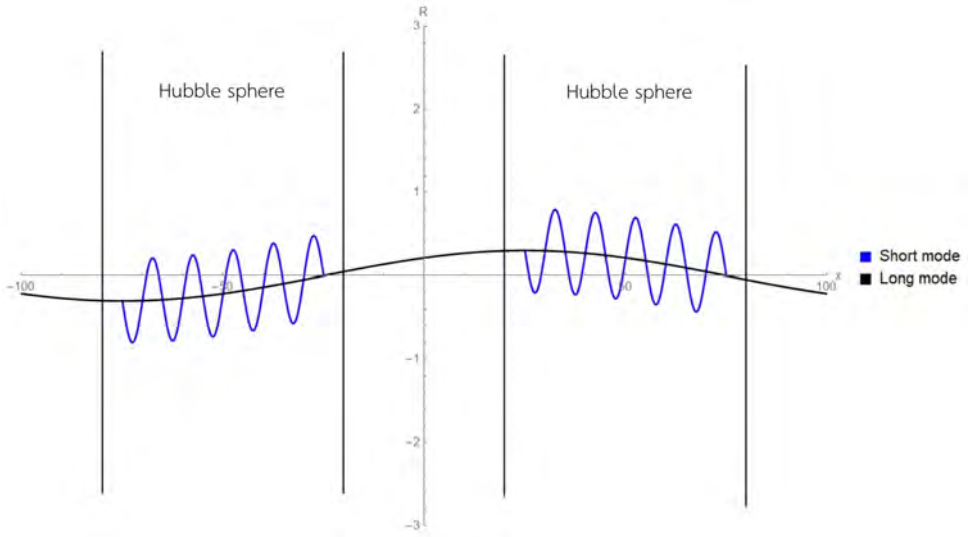

Figure 10: A Visualization of the short modes correlated with the frozen long mode. Those two short modes are still evolving deeply in its horizon (Hubble sphere) while the frozen mode is already far outside and becomes a part of the background.

the long mode perturbation. For convenient, the long and short mode variables are subscripted by L and S. Let us recall the definition of the spectral index (4.5.13), $n_s - 1 \equiv \frac{d\ln k^3 P_{\mathcal{R}}}{d\ln k}$, from the previous section to present the scale-dependence of the curvature power spectrum in the single-field inflation. We are going to start off with the two-point function in x space, $\langle \mathcal{R}_S(\vec{x})\mathcal{R}_S(\vec{x}+\vec{r})\rangle_L$. This function can be Taylor expanded as

$$\langle \mathcal{R}_S(\vec{x})\mathcal{R}_S(\vec{x}+\vec{r})\rangle_L = \langle \mathcal{R}_S(\vec{x})\mathcal{R}_S(\vec{x}+\vec{r})\rangle_0 + \delta\vec{r}\cdot\vec{\nabla}_r\langle \mathcal{R}_S(\vec{x})\mathcal{R}_S(\vec{x}+\vec{r})\rangle_0 + \mathcal{O}(2), \tag{6.0.2}$$

where $\langle \mathcal{R}_S(\vec{x})\mathcal{R}_S(\vec{x}+\vec{r})\rangle_0$ is the value where $\mathcal{R}_L$ is absent. Note that we can perform the expansion above because the perturbations from the long mode is small. We have already argued that this function is a homogeneous function on x-space. Thus, the reference point $\vec{x}$ is arbitrary. Also, the output is isotropic since the function yields a scalar quantity. Hence, the two-point function depends on $|\vec{r}|$ only,

$$\langle \mathcal{R}_S(\vec{x})\mathcal{R}_S(\vec{x}+\vec{r})\rangle_0 = \xi(|\vec{r}|). \tag{6.0.3}$$

The function $\xi(|\vec{r}|)$ is introduced to represent the two-point function for convenient. By keeping the perturbation up to the linear order, the Taylor expansion reduces to

$$\langle \mathcal{R}_S(\vec{x})\mathcal{R}_S(\vec{x}+\vec{r})\rangle_L = \xi(|\vec{r}|) + \delta r\frac{d}{dr}\xi(|\vec{r}|). \tag{6.0.4}$$

Next, let us consider the spatial coordinates disturbances due to long mode curvature perturbation. From the perturbed metric (4.2.1), one can see that the transformed coordinate (denoted with prime) is written as

$$d\vec{x}' = e^{\mathcal{R}_L}d\vec{x}. \tag{6.0.5}$$

Here, the small displacement $d\vec{x}$ has been re-scaled by the frozen disturbance. Thus, the coordinates transform as

$$x^{i\prime} = \frac{dx^{i\prime}}{dx^j}x^j = e^{\mathcal{R}_L}\delta^i_j x^j = (1+\mathcal{R}_L+\mathcal{O}(\mathcal{R}^2))x^i.$$

In this transformation, we kept the perturbation $\mathcal{R}_L$ up to the linear order. Therefore, the curvature

disturbance here induced the coordinate transformation such that

$$\vec{r} \longrightarrow \vec{r}' = \vec{r} + \mathcal{R}_L \vec{r}. \tag{6.0.6}$$

That is, any length scales on the background are stretched or contracted by the long mode by $\delta r = \mathcal{R}_L r$. By substituting it into (6.0.4), one gets

$$\left\langle \mathcal{R}_S(\vec{x})\mathcal{R}_S(\vec{x}+\vec{r}) \right\rangle_L = \xi(|\vec{r}|) + \mathcal{R}_L r \frac{d}{dr}\xi(|\vec{r}|). \tag{6.0.7}$$

To match the result with the formula (5.0.13), the relation should be presented in Fourier space. One can Fourier transform the equation and gets the perturbed two-point function in k-space:

$$\left\langle \mathcal{R}_S(\vec{k_1})\mathcal{R}_S(\vec{k_2}) \right\rangle_L = \delta^{(3)}(\vec{k_1}+\vec{k_2})\left[P_S(|\vec{k_1}|) - \mathcal{R}_L P_S(|\vec{k_1}|)\frac{d\ln k_1^3 P_S(|\vec{k_1}|)}{d\ln k_1} \right]. \tag{6.0.8}$$

The power spectrum depends on one of the k-vectors only since $\vec{k_1} \approx \vec{k_2}$ in this case. From (4.5.12), one find that the equation is

$$\left\langle \mathcal{R}_S(\vec{k_1})\mathcal{R}_S(\vec{k_2}) \right\rangle_L = \delta^{(3)}(\vec{k_1}+\vec{k_2})\left[P_S(|\vec{k_1}|) + (1-n_s)\mathcal{R}_L P_S(|\vec{k_1}|) \right]. \tag{6.0.9}$$

By substituting the relation into the equation (6.0.1), one gets

$$\left\langle \mathcal{R}_S(\vec{k_1})\mathcal{R}_S(\vec{k_2})\mathcal{R}_L(\vec{k_3}) \right\rangle = (2\pi)^3\delta^{(3)}(\vec{k_1}+\vec{k_2}+\vec{k_3})(1-n_s)P_S(|\vec{k_1}|)P_L(|\vec{k_3}|). \tag{6.0.10}$$

Finally, from the equation above with the definition of the bispectrum, one gets the *single field consistency condition* or the *single-field theorem*:

$$B_{\mathcal{R}}(|\vec{k_1}|,|\vec{k_2}|,|\vec{k_3}| \to 0) = (1-n_s)P_{\mathcal{R}}(|\vec{k_1}|)P_{\mathcal{R}}(|\vec{k_3}|). \tag{6.0.11}$$

The theorem states that the relation must hold for all single-field inflation models. It is important to emphasize that this is true only if inflaton is the only field. As mentioned before, the curvature disturbance on each point can be considered as if some points inflate more or less than the background (see subsection 4.2). This is equivalent to the coordinates re-scaling done earlier. Thus, the contribution from the long mode can be directly considered as the re-scaling, or equivalently, changing the horizon crossing time. Hence, the power spectrum will be affected due to its scale dependency. However, by introducing the second field, the relation between long mode and the reparameterized scale factor is not exact as before. Namely, the transformation (6.0.6) will be wrong. This is because there will be more than one degree of freedom contributed to the curvature fluctuation. Thus, the argument above breaks down for multi-field inflation.

The result here links the local-form non-Gaussianity with the scale-dependency of the power spectrum. If we recall the (5.0.13) and take it to the squeezed limit, the nonlinear parameter f_{NL} in the squeezed limit for single-field inflation is written as

$$f_{NL} = \frac{5}{12}(1-n_s). \tag{6.0.12}$$

Both f_{NL} and n_s can be measured by different methods. Therefore, the relation can be checked by the observations. From [6], the spectral index constrains the parameter f_{NL} to around the order of 10^{-2}, which implies a tiny squeezed bispectrum compared to the square of the power spectrum. Since the power spectrum is observably small by itself (in the order of fluctuations squared or 10^{-9}), the squeezed bispectrum thus too small to be detected nowadays. The readers might wonder how can we confirm the prediction if it is too tiny to detect. But actually, the point of this condition is how easy and powerful the violation of it is. As mentioned before, the parameter f_{NL} can be large enough to

be detectable. This means it is possible to find the squeezed bispectrum in the observation. This will violate the condition and automatically rule out every single-field model, despite its detail whatsoever. As mentioned, the spectral index and the nonlinear parameter for this local non-Gaussianity are measured as $n_s = 0.9649 \pm 0.0042$ and $f_{NL} = -0.9 \pm 5.1$, both with 68% CL. [6, 7]. Thus, the single-field models have not been ruled out until now. However, many surveys promise to measure this parameter with more precision. Thus, there are still possibilities that all single-field models will be ruled out in the future.

7. The Four-point Function

From the previous section, the correction terms were computed up to the third order. There, we obtain the single-field consistency relation, which can teach us about the number of fields in inflation. In this section, we shall move on to the four-point correlation function. Similar to the last section, not only that the function serves as a correction to the PDF, it also tells us about some aspects of inflationary model as we are going see shortly. Let us recall the equation (5.0.5). The procedures are quite the same, we are going compute the four-point function of the non-local form $\mathcal{R}$ in Fourier space (for more details, see Appendix A). A well-organized computation is provided by Teruaki Suyama and Masahide Yamaguchi [23]. In the paper, the terms with first-order f_{NL} vanished since they are consisted with the three-point functions of the Gaussian variable. Thus, we would like to include the next parameters g_{NL} now. Like before, we are allowed to compute up to linear order of the parameters only. This is because the squared parameters and higher-orders are tiny compared to the leading term and hence negligible. The result is

$$\begin{aligned}\left\langle \mathcal{R}(\vec{k_1})\mathcal{R}(\vec{k_2})\mathcal{R}(\vec{k_3})\mathcal{R}(\vec{k_4})\right\rangle =&(2\pi)^3\Big\{\delta^{(3)}(\vec{k_1}+\vec{k_2})\delta^{(3)}(\vec{k_3}+\vec{k_4})P_{\mathcal{R}}(|\vec{k_1}|)P_{\mathcal{R}}(|\vec{k_3}|)+\text{perm}(2,3,4)\Big\}\\ &+(2\pi)^3\delta^{(3)}(\vec{k_1}+\vec{k_2}+\vec{k_3}+\vec{k_4})\Big\{\\ &\frac{54}{25}g_{NL}\Big[P_{\mathcal{R}}(|\vec{k_1}|)P_{\mathcal{R}}(|\vec{k_2}|)P_{\mathcal{R}}(|\vec{k_3}|)+\text{perm}(1,2,3,4)\Big]\\ &+\tau_{NL}\Big[P_{\mathcal{R}}(|\vec{k_3}|)P_{\mathcal{R}}(|\vec{k_4}|)\big[P_{\mathcal{R}}(|\vec{k_1}+\vec{k_3}|)+P_{\mathcal{R}}(|\vec{k_1}+\vec{k_4}|)\big]+\text{perm}(1,2,3,4)\Big]\Big\}.\end{aligned} \tag{7.0.1}$$

The nonlinear parameter τ_{NL} is introduced to present the contribution of the third term. As done with the bispectrum, we would like to measure those nonlinear parameters for the PDF correction. But, the contributions from those three terms in the formula are mixed. Hence, we need to find a way to investigate them separately. Since we have the freedom to choose the configuration of those four mode vectors of trispectrum, we will consider some configurations by which we can investigate the terms separately. As mentioned before, the power spectrum peaks when the norm of the mode vector approaches zero. This means each term on the right side of the equation peaks at a different limit. Therefore, we can measure and study each contribution separately.

For convenience, we would like to define the magnitude of the four-point function associated with the mode vectors, the *trispectrum*, as

$$\left\langle \mathcal{R}(\vec{k_1})\mathcal{R}(\vec{k_2})\mathcal{R}(\vec{k_3})\mathcal{R}(\vec{k_4})\right\rangle = (2\pi)^3\delta^{(3)}(\vec{k_1}+\vec{k_2}+\vec{k_3}+\vec{k_4})T_{\mathcal{R}}(|\vec{k_1}|,|\vec{k_2}|,|\vec{k_3}|,|\vec{k_4}|). \tag{7.0.2}$$

First of all, the four-point function holds some value only if all of the mode vectors sum to null vector. Namely, they form a quadrilateral (see Figure 11). This came from the fact that the four-point is required to be a homogeneous function over x-space; it holds the same value despite the position on CMB map. Next, we are going to investigate the limits where each term peaks [41]. If we consider the limit where one of the mode vector is tiny compared to others, the most contribution comes from the term with g_{NL}. In this limit, the first and third term are neglected by the constraint of delta

functions and a sufficiently small value. Therefore, the parameter can be estimate from the formula[4]:

$$\frac{54}{25}g_{NL} = \frac{T_{\mathcal{R}}(|\vec{k_1}|,|\vec{k_2}|,|\vec{k_3}|,|\vec{k_4}|)}{P_{\mathcal{R}}(|\vec{k_1}|)[P_{\mathcal{R}}(|\vec{k_2}|)P_{\mathcal{R}}(|\vec{k_3}|)+\text{perm}(2,3,4)}, \tag{7.0.3}$$

where $|\vec{k_2}|,|\vec{k_3}|,|\vec{k_4}| \gg |\vec{k_1}| \longrightarrow 0$ in this squeezed limit. On another hand, the term with τ_{NL} peaks at the small diagonal limit. In this limit, one of the quadrilateral diagonal lines is squeezed in causing the power spectrum to peak (see Figure 11). For instance, $P_{\mathcal{R}}(|\vec{k_1}+\vec{k_3}|)$ peaks when $|\vec{k_1}+\vec{k_3}| \longrightarrow 0$. Now, the other terms are tiny regarding the second term and hence negligible. Therefore, the parameter can be computed from the following formula

$$\tau_{NL} = \frac{T_{\mathcal{R}}(|\vec{k_1}|,|\vec{k_2}|,|\vec{k_3}|,|\vec{k_4}|)}{P_{\mathcal{R}}(|\vec{k_3}|)P_{\mathcal{R}}(|\vec{k_4}|)P_{\mathcal{R}}(|\vec{k_1}+\vec{k_3}|)+\text{perm}(2,3,4)}. \tag{7.0.4}$$

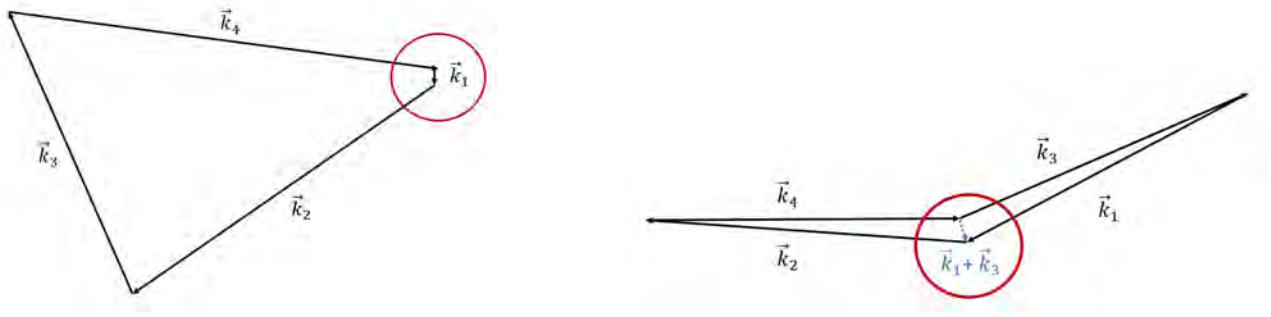

(a) The squeezed trispectrum *(b) The small diagonal trispectrum*

Figure 11: The quadrilateral of the trispectrum mode vectors at the peak limits. The subfigure (a) present the squeezed trispectrum correspond to peak of the term with g_{NL}. In the subfigure (b), the trispectrum is at small diagonal limit correspond to peak of τ_{NL} term.

In addition, this parameter has another interesting feature other than being a part of the correction. That is, a large group of the inflationary models can be eliminated by the measurement of τ_{NL}. Suppose all single-field models are ruled out from the violation of (6.0.12), there is still a huge number of multi-field models that are theoretically allowed. To specify the exact model, it would be nice to scope down even more. The study shows that the parameters τ_{NL} and f_{NL} are related via the *Suyama-Yamaguchi inequality* [23]:

$$\tau_{NL} \geq \left(\frac{6}{5}f_{NL}\right)^2. \tag{7.0.5}$$

This is also known as the *multi-field consistency relation*. In other words, the leading contribution of the non-Gaussianity comes from the four-point function rather than the three-point function. The minimum case where $\tau_{NL} = \left(\frac{6}{5}f_{NL}\right)^2$ corresponds to the single-field scenario (see Appendix A). In 2011, the relation is generalized by Naonori S. Sugiyama, Eiichiro Komatsu and Toshifumi Futamase [25]. In summary, we have another relation to test inflation. When the condition is violated, the model is no longer valid if it assumes the following: First, the source of primordial fluctuation comes from the field disturbance only. Secondly, the individual mode of fluctuations that exited the horizon is scale-invariant and Gaussian distributed. Lastly, the overall deviation from Gaussian statistics must be small so that the perturbative approach to non-Gaussianity is allowed. Also, the leading contribution of it must be the power series ansatz (5.0.5). Just to remind the readers, these are the conditions imposed along in the discussion until now, from the source of fluctuations to the computation of

[4]To be precise, there is mixed contribution from the τ_{NL} term in this limit as well, but in a predictable fashion. Hence, the formula is not exact but the idea is roughly along this line. A full description about it is provided in [41].

non-Gaussianity. To be precise, most of these assumptions are the mechanisms provided naturally by inflation. Thus, there is a chance that it is not where the primordial fluctuation originates from if the relation is falsified.

Similar to the single-field theorem, these parameters on each side, f_{NL} and τ_{NL} in this case, can be measured from separate methods. Thus, this consistency relation can be judged by comparing these separately measured parameters. Also, we are interested in the violation of it. For instance, the models where field fluctuations are the only source of non-Gaussianity will be ruled out. The paper [25] also mentioned a lot more mechanisms that might be ruled out by the violation. Thus, this has the potential to rule out a large class of multi-field model with the mentioned mechanisms. Recent measurement by Planck satellite provided $g_{NL} = (-5.8 \pm 6.5) \times 10^4$ with 68% CL., statistically. Also, we have already mentioned the measurement of $f_{NL} = -0.9 \pm 5.1$ with the same confidence level of the error bar. With this measurement, the parameter τ_{NL} is expected to be equal to or greater than 16 approximately.

8. The Higher n-point Functions

As we have mentioned in section 5, the perturbation function $f(\mathcal{R}_g)$ reflects the additional features in the true model. Here, the form of perturbation function corresponds to the feature of interest. Previously, we are interested in the power-law potential and investigate the power-law form of the perturbation. We have computed the correction terms up to fourth-order (the four-point function). One could stop here by assuming that the parameters converge at sufficiently high-order of perturbation. This is normally the case of the potential with power-law form in the Lagrangian. However, there are cases where the parameters do not converge in high-order. For example, the case where the perturbation $f(\mathcal{R}_g)$ is a periodic function, like sine and cosine. To have a visible periodic behaviour, one must keep numerous, if not all, terms of the Taylor expansion. The case exists if we include the *axion*[5] in our theory. This is because axion has a sinusoidal potential which will give the non-Gaussian signature as a sinusoidal form (see Figure 12) [26, 27]. Besides, all of the odd-order point functions vanished. This is because the PDF curve is still symmetric about its zero mean as shown in Figure 12. This means the parameter f_{NL} will be measured as zero even if the PDF is perturbed.

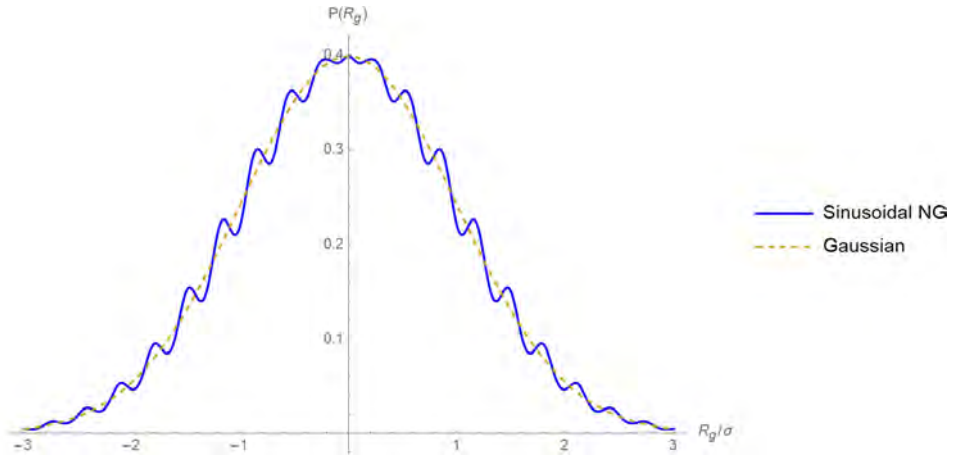

Figure 12: The probability density function curve when the perturbation term is a sine function. Based on the perturbative method, this is the kind of non-Gaussianity that requires a large number of n-point functions to capture, which is inefficient if even possible.

For the reasons mentioned above, this kind of non-Gaussianity obviously cannot be characterized with the two-, three- or four-point functions, which are the furthest measurable data until now. This is because the accuracy is not enough to probe higher n-point functions. Generally speaking, we measure the n-point function by counting the group of n data points with equal temperature separated by specific distances. Since the number of data points is limited, the higher order of n-point function we probe, the fewer data to measure. Namely, for finite data points, one can form less groups of n data points when n is bigger. For instance, there are more pairs of points to measure the two-point function than groups of three points to measure the three-point function in the CMB map (See Figure 13). For this reason, the current data is not enough to justify the acceptable value of higher n-point functions. It would require more investments and higher technologies to measure enough n-point functions for this non-Gaussianity characterization. Thus, we are constrained by the power of satellites and observatories. Also, the computation of the higher n-point function seems to be more complicated. For the above reasons, the set of low n-point functions may not be suited to

[5]Axion is a hypothetical particle proposed to resolve a problem in quantum chromodynamics (QCD).

some classes of non-Gaussian signatures, like the sine function mentioned above. Hence, one might be tempted to find alternative methods that also can reveal the full PDF of the CMB fluctuations.

Just to mention one such statistical estimator, the *Minkowski functional* is a direct probe to the full PDF, which is model-independent [42]. The functional returns a specific real number for the corresponding form of PDF. Namely, the functional return a real number for a Gaussian PDF and a different number for a non-Gaussian PDF. The returned number is measurable and is used to justify the exact form of the PDF. However, there is no certain answer until now. This is one of the open questions that are currently active in the field of study.

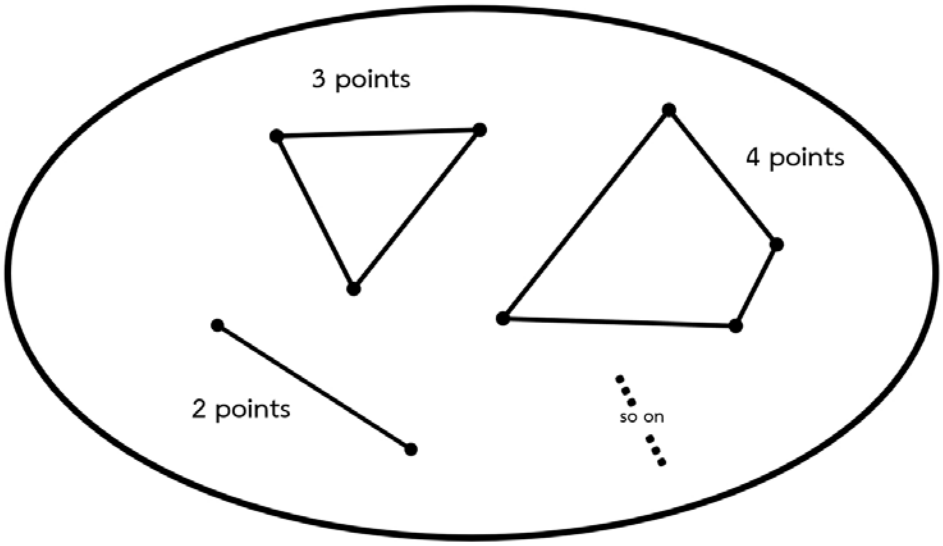

Figure 13: Illustration of the n-point functions probe on the CMB sky. Broadly speaking, it would require n separated pixels in the temperature map to form a group of data. For instance, the two-point function requires 2 data points and the three-point function requires 3 data points in this picture. Generally, more groups of data mean high accuracy and the measurement will be more acceptable. Thus, the estimation of the n-point functions will be less justifiable by increasing n for finite data points.

9. Conclusion

In this project, we discussed the statistics of the CMB temperature fluctuations and how they relate to the physics of inflation. The discussion opened up with some background and motivation for the inflationary model of the very early universe. Then, we describe the physics that drove this era. We argue that the form of CMB temperature fluctuations is evidence of the density fluctuations in inflation. Thus, the statistics of the fluctuations is a perfect window into the physics of inflation. This came from the fact that the form of probability density function (PDF) of the fluctuations is determined by the action of it. By knowing the full PDF of the CMB fluctuations, one can write the full action of the matter component in inflation. At the starting point, the simplest model proposed a scalar field, the inflaton, that drives inflation. The study shows that this simplest model gives normally distributed fluctuations to the CMB.

The observations [6] seem to confirm the prediction from the simplest model but also allow for small deviations. Hence, the actual model might not be so simple as proposed. This hypothesis is well-motivated since we expect the theory to be more complicated at very high energy. Since inflation occurs when the space is very tight, the energy density must indeed be very high. For the sake of comparison, the lower-bound energy scale of inflation is significantly greater than the collisions at LHC. Thus, detection of non-Gaussianity could lead to the discovery of new physics that cannot be achieved by any particle colliders nowadays. Besides, there are still many aspects of inflation that remain uncertain until now. One of the fundamental questions discussed in this project is "how many fields are active during inflation?". The finding of the departure from normal distribution might be able to fix those fundamental aspects, or at least gives some clues about it. This overall initiates the study of non-Gaussianity of the CMB fluctuations to learn more about inflation.

To study the small departure from Gaussian distribution, we applied the perturbation theory to its PDF. Normally, the odd-order n-point correlation functions vanish for the Gaussian distribution. Hence, a certain detection of those functions indicates some deviation from it. For example, a non-zero three-point function introduces skewness to the distribution (see Figure 8). In this context, the n-point correlation functions serve as corrections to the PDF. Therefore, they are the things to measure from the observations. Here, we showed the theoretical formulae of these functions based on the aspect of interest, i.e. a power series interaction. In this case, the three- and four-point functions can be written in terms of two-point functions. We can use these formulae to determine the correction term from the measured correlation functions. We also learn that these functions have their peak limits at which they are probed, for instance, the squeezed limit (see section 6). Furthermore, these functions are related to the fundamental aspects of the inflationary model as mention before. The magnitude of the three-point function can justify if the single-field models are valid or not. This is the so-called single-field consistency relation. A large enough signal of this function has the potential to exclude all single-field models from the candidates. Another noteworthy relation is the multi-field consistency relation. The relation states that the magnitude of the four-point function can be used to test the process of generating fluctuations during inflation. Again, the violation of this relation can exclude a large class of multi-field models that generate the fluctuations via the processes mentioned in this statement.

Finally, we explained that the higher n-point function is hard to achieve both in theoretical and observational ways. In the context of perturbation theory, it will require a lot of n-point functions to characterize some forms of deviation from the Gaussian, for example, the sine function. This is because we need to keep the power-law expansion terms up to sufficiently large order for the periodic behaviour of it, hence many correction terms are essential. Unfortunately, the highest n-point function that we could probe nowadays is the four-point function due to the observational limit. Until now, not only the measured n-point functions are not enough to characterize this form of deviation, none

of the measurements is good enough to confirm the existence of non-Gaussianity in general. However, since the idea is so well-motivated from the mentioned reasons, there might be other forms of the departure that cannot be observed via the three- and four-point functions. Hence, the existence of those departures cannot be confirmed via the correlation functions measured by the surveys up until now. Hence, a new approach to reveal the actual statistics is convincing.

Soon, many surveys promise to deliver the CMB data with more accuracy. One of the collaborations is the CMB-S4 [43], which is a group of ground-based telescopes distributed around the globe. This will help to remove the contamination of other galactic objects, which is promising for more accurate results. Another approach to the statistics of the primordial fluctuations is the large-scale structure, which refers to the universe's configuration in a scale much larger than an individual galaxy, e.g., a cluster of galaxies. As mentioned in the introduction, the fluctuations observed in the CMB map also seed the structure formation, thus the statistics of the CMB is also reflected in the statistics of the large-scale structure. Although the data from this approach is very complicated to analyse, the data map will be three-dimensional in return. Unlike the CMB map, which is two-dimensional, the statistics in this map might reveal some new information about the primordial fluctuations and lead to more understanding of the physics during inflation. One of the projects that can achieve this generous kind of data is the Square Kilometre Array (SKA) project [44]. With more accurate data in the future, physicists can learn more about our universe at a very early time and physics at a high energy scale.

References

[1] A. Friedman, "On the Curvature of space", Z. Phys. **10**, 377–386 (1922).

[2] G. Lemaitre, "A Homogeneous Universe of Constant Mass and Growing Radius Accounting for the Radial Velocity of Extragalactic Nebulae", Annales Soc. Sci. Bruxelles A **47**, 49–59 (1927).

[3] P. J. E. Peebles, "Recombination of the Primeval Plasma", Astrophys. J. **153**, 1 (1968).

[4] Planck Collaboration (Planck), "Planck 2018 results. I. Overview and the cosmological legacy of Planck", Astron. Astrophys. **641**, A1 (2020).

[5] Planck Collaboration, "Planck 2018 results. V. CMB power spectra and likelihoods", Astron. Astrophys. **641**, A5 (2020).

[6] Planck Collaboration, "Planck 2018 results. X. Constraints on inflation", Astron. Astrophys. **641**, A10 (2020).

[7] Planck Collaboration, "Planck 2018 results. IX. Constraints on primordial non-Gaussianity", Astron. Astrophys. **641**, A9 (2020).

[8] A. H. Guth, "The Inflationary Universe: A Possible Solution to the Horizon and Flatness Problems", Phys. Rev. D **23**, 347–356 (1981).

[9] A. A. Starobinsky, "A New Type of Isotropic Cosmological Models Without Singularity", Adv. Ser. Astrophys. Cosmol. **3**, 130–133 (1987).

[10] A. D. Linde, "A New Inflationary Universe Scenario: A Possible Solution of the Horizon, Flatness, Homogeneity, Isotropy and Primordial Monopole Problems", Phys. Lett. B **108**, 389–393 (1982).

[11] A. Albrecht and P. J. Steinhardt, "Cosmology for Grand Unified Theories with Radiatively Induced Symmetry Breaking", Phys. Rev. Lett. **48**, 1220–1223 (1982).

[12] V. F. Mukhanov and G. V. Chibisov, "Quantum Fluctuations and a Nonsingular Universe", JETP Lett. **33**, 532–535 (1981).

[13] A. H. Guth and S. Y. Pi, "Fluctuations in the New Inflationary Universe", Phys. Rev. Lett. **49**, 1110–1113 (1982).

[14] S. W. Hawking, "The Development of Irregularities in a Single Bubble Inflationary Universe", Phys. Lett. B **115**, 295 (1982).

[15] A. A. Starobinsky, "Dynamics of Phase Transition in the New Inflationary Universe Scenario and Generation of Perturbations", Phys. Lett. B **117**, 175–178 (1982).

[16] J. M. Bardeen, P. J. Steinhardt, and M. S. Turner, "Spontaneous Creation of Almost Scale - Free Density Perturbations in an Inflationary Universe", Phys. Rev. D **28**, 679 (1983).

[17] N. Bartolo, E. Komatsu, S. Matarrese, and A. Riotto, "Non-Gaussianity from inflation: Theory and observations", Phys. Rept. **402**, 103–266 (2004).

[18] E. Komatsu and D. N. Spergel, "Acoustic signatures in the primary microwave background bispectrum", Phys. Rev. D **63**, 063002 (2001).

[19] G. A. Palma, B. Scheihing Hitschfeld, and S. Sypsas, "Non-Gaussian CMB and LSS statistics beyond polyspectra", JCAP **02**, 027 (2020).

[20] T. Suyama and S. Yokoyama, "Statistics of general functions of a Gaussian field -application to non-Gaussianity from preheating-", JCAP **06**, 018 (2013).

[21] J. Ganc and E. Komatsu, "A new method for calculating the primordial bispectrum in the squeezed limit", JCAP **12**, 009 (2010).

[22]P. Creminelli and M. Zaldarriaga, "Single field consistency relation for the 3-point function", JCAP **10**, 006 (2004).

[23]T. Suyama and M. Yamaguchi, "Non-Gaussianity in the modulated reheating scenario", Phys. Rev. D **77**, 023505 (2008).

[24]C. T. Byrnes, M. Sasaki, and D. Wands, "The primordial trispectrum from inflation", Phys. Rev. D **74**, 123519 (2006).

[25]N. S. Sugiyama, E. Komatsu, and T. Futamase, "Non-Gaussianity Consistency Relation for Multi-field Inflation", Phys. Rev. Lett. **106**, 251301 (2011).

[26]X. Chen, G. A. Palma, W. Riquelme, B. Scheihing Hitschfeld, and S. Sypsas, "Landscape tomography through primordial non-Gaussianity", Phys. Rev. D **98**, 083528 (2018).

[27]X. Chen, G. A. Palma, B. Scheihing Hitschfeld, and S. Sypsas, "Reconstructing the Inflationary Landscape with Cosmological Data", Phys. Rev. Lett. **121**, 161302 (2018).

[28]A. R. Liddle, P. Parsons, and J. D. Barrow, "Formalizing the slow roll approximation in inflation", Phys. Rev. D **50**, 7222–7232 (1994).

[29]L. Kofman, A. D. Linde, and A. A. Starobinsky, "Towards the theory of reheating after inflation", Phys. Rev. D **56**, 3258–3295 (1997).

[30]L. Kofman, A. D. Linde, and A. A. Starobinsky, "Reheating after inflation", Phys. Rev. Lett. **73**, 3195–3198 (1994).

[31]J. M. Bardeen, "Gauge Invariant Cosmological Perturbations", Phys. Rev. D **22**, 1882–1905 (1980).

[32]V. F. Mukhanov, H. A. Feldman, and R. H. Brandenberger, "Theory of cosmological perturbations. Part 1. Classical perturbations. Part 2. Quantum theory of perturbations. Part 3. Extensions", Phys. Rept. **215**, 203–333 (1992).

[33]V. F. Mukhanov, H. A. Feldman, and R. H. Brandenberger, "Theory of cosmological perturbations. Part 1. Classical perturbations. Part 2. Quantum theory of perturbations. Part 3. Extensions", Phys. Rept. **215**, 203–333 (1992).

[34]D. H. Lyth, K. A. Malik, and M. Sasaki, "A General proof of the conservation of the curvature perturbation", JCAP **05**, 004 (2005).

[35]T. S. Bunch and P. C. W. Davies, "Quantum Field Theory in de Sitter Space: Renormalization by Point Splitting", Proc. Roy. Soc. Lond. A **360**, 117–134 (1978).

[36]C. Kiefer, D. Polarski, and A. A. Starobinsky, "Quantum to classical transition for fluctuations in the early universe", Int. J. Mod. Phys. D **7**, 455–462 (1998).

[37]G. W. Gibbons and S. W. Hawking, "Cosmological Event Horizons, Thermodynamics, and Particle Creation", Phys. Rev. D **15**, 2738–2751 (1977).

[38]A. R. Liddle and D. H. Lyth, "COBE, gravitational waves, inflation and extended inflation", Phys. Lett. B **291**, 391–398 (1992).

[39]R. K. Sachs and A. M. Wolfe, "Perturbations of a cosmological model and angular variations of the microwave background", Astrophys. J. **147**, 73–90 (1967).

[40]J. M. Maldacena, "Non-Gaussian features of primordial fluctuations in single field inflationary models", JHEP **05**, 013 (2003).

[41]A. Lewis, "The real shape of non-gaussianities", Journal of Cosmology and Astroparticle Physics **2011**, 026–026 (2011).

[42]T. Buchert, M. J. France, and F. Steiner, "Model-independent analyses of non-Gaussianity in Planck CMB maps using Minkowski functionals", Class. Quant. Grav. **34**, 094002 (2017).

[43]CMB-S4 Collaboration, *CMB-S4 decadal survey apc white paper*, (2019) https://arxiv.org/abs/1908.01062, (arXiv:1908.01062).

[44]D.C.-J.Bock, P.E.Dewdney, S.T.Garrington, J.Horrell, R.Vermeulen, and A.Wicenec, *Concept of operations for the ska observatory*, (2013) https://www.skatelescope.org/wp-content/uploads/2011/03/SKAConOpsRevB.pdf.

Appendix A. Computation of the Four-point Function

We will go through the computation of the four-point function to obtain the result in section 7 in the single field scenario. The procedures and ideas are quite the same as the three-point function computed in the section 5. That is, we assume that the source of fluctuations is the inflaton disturbance only, each mode of fluctuations exited the horizon being scale-invariant and Gaussian and the power-law perturbation terms are the leading contribution to the non-Gaussianity (see section 4). First, let us recall the perturbed variables (5.0.5):

$$\mathcal{R}(\vec{x}) = \mathcal{R}_g(\vec{x}) + \frac{3}{5} f_{NL}(\mathcal{R}_g^2(\vec{x}) - \langle \mathcal{R}_g^2(\vec{x}) \rangle) + \frac{9}{25} g_{NL} \mathcal{R}_g^3(\vec{x}) + \dots \,, \tag{A.1}$$

and in Fourier space (5.0.6):

$$\begin{aligned} \mathcal{R}(\vec{k}) =& \mathcal{R}_g(\vec{k}) + \frac{3}{5} f_{NL} \int \frac{d^3k'}{(2\pi)^3} \Big[\mathcal{R}_g(\vec{k}') \mathcal{R}_g(\vec{k} - \vec{k}') - \langle \mathcal{R}_g(\vec{k}') \mathcal{R}_g(\vec{k} - \vec{k}') \rangle \Big] \\ &+ \frac{9}{25} g_{NL} \int \frac{d^3k'}{(2\pi)^3} \int \frac{d^3k''}{(2\pi)^3} \Big[\mathcal{R}_g(\vec{k}'') \mathcal{R}_g(\vec{k}') \mathcal{R}_g(\vec{k} - \vec{k}' - \vec{k}'') \Big] + \dots \,. \end{aligned} \tag{A.2}$$

Here, we keep the perturbation terms up to the parameter g_{NL} because the term with first-order f_{NL} will vanish in the computation that will be shown shortly. Next, we obtain the four-point function by computing the correlation between four distinct duplicated of this variable:

$$\begin{aligned} \langle \mathcal{R}(\vec{k_1}) \mathcal{R}(\vec{k_2}) \mathcal{R}(\vec{k_3}) \mathcal{R}(\vec{k_4}) \rangle =& \langle \mathcal{R}_g(\vec{k_1}) \mathcal{R}_g(\vec{k_2}) \mathcal{R}_g(\vec{k_3} \mathcal{R}(\vec{k_4})) \rangle \\ &+ \frac{9}{25} g_{NL} \Big[\Big\langle \int \frac{d^3k_1'}{(2\pi)^3} \int \frac{d^3k_1''}{(2\pi)^3} \Big[\mathcal{R}_g(\vec{k_1}'') \mathcal{R}_g(\vec{k_1}') \mathcal{R}_g(\vec{k_1} - \vec{k_1}' - \vec{k_1}'') \mathcal{R}_g(\vec{k_2}) \mathcal{R}_g(\vec{k_3}) \mathcal{R}_g(\vec{k_4}) \Big\rangle + \text{perm.} \Big] \\ &+ \frac{9}{25} f_{NL}^2 \Big[\Big\langle \int \frac{d^3k_1'}{(2\pi)^3} \int \frac{d^3k_2'}{(2\pi)^3} \Big[\mathcal{R}_g(\vec{k_1}') \mathcal{R}_g(\vec{k_1} - \vec{k_1}') - \langle \mathcal{R}_g(\vec{k_1}') \mathcal{R}_g(\vec{k_1} - \vec{k_1}') \rangle \Big] \\ &\Big[\mathcal{R}_g(\vec{k_2}') \mathcal{R}_g(\vec{k_2} - \vec{k_2}') - \langle \mathcal{R}_g(\vec{k_2}') \mathcal{R}_g(\vec{k_2} - \vec{k_2}') \rangle \Big] \mathcal{R}_g(\vec{k_3}) \mathcal{R}_g(\vec{k_4}) \rangle + \text{perm.} \Big]. \end{aligned}$$

If one follows the multiplication above, one can see that the term with first-order f_{NL} consists of products of three-point of Gaussian variable. Hence, the term vanishes and leaves the main contribution to g_{NL} and f_{NL}^2. For neatness, each term will be computed separately.

We will start with the first term, which is the four-point function of the Gaussian variables. As usual, we can expand it into products of two-point functions via the Wick's theorem. Then, the functions can be substituted by the definition of the power spectrum (5.0.8): $\langle \mathcal{R}_g(\vec{k}) \mathcal{R}_g(\vec{k}') \rangle = (2\pi)^3 \delta^{(3)}(\vec{k} + \vec{k}') P_{\mathcal{R}}(|\vec{k}|)$. Thus, the first term becomes

$$\langle \mathcal{R}_g(\vec{k_1}) \mathcal{R}_g(\vec{k_2}) \mathcal{R}_g(\vec{k_3} \mathcal{R}(\vec{k_4})) \rangle = (2\pi)^3 \Big\{ \delta^{(3)}(\vec{k_1} + \vec{k_2}) \delta^{(3)}(\vec{k_3} + \vec{k_4}) P_{\mathcal{R}}(|\vec{k_1}|) P_{\mathcal{R}}(|\vec{k_3}|) + \text{perm}(2,3,4) \Big\}.$$

In terms of new implication, this contribution is not what we are interested in. This is because it will have some non-zero value only when the quadrilateral of mode vectors degenerate to two-line or the small diagonal limit as shown in Figure 11. But, the third term peaks at that limit as mentioned in section 7. Thus, even in the scenario where the term holds some value, it is insignificant compared to other terms anyway.

Next is the g_{NL} term. Since the terms repeat themselves with permuted $\vec{k}$, we will compute one of the permutation term only. It can be simplified as following: First, we expand the six-point function in the integral by using the Wick's Theorem. Then, it becomes products of power spectra. By integrating all terms, the end result is

$$\text{one in the second term} = 6(2\pi)^3\delta^{(3)}(\vec{k_1}+\vec{k_2}+\vec{k_3}+\vec{k_4})P_{\mathcal{R}}(|\vec{k_2}|)P_{\mathcal{R}}(|\vec{k_3}|)P_{\mathcal{R}}(|\vec{k_4}|).$$

The last one is the terms with f_{NL}^2. Here, the procedures repeat from the previous one. By considering one of the permutation terms, we expands the six-point function via Wick's Theorem. The negative two-point functions will cancel out some of the terms. Then, we further simplify the expression and integrate $\vec{k_1}'$ and $\vec{k_1}''$ out. The result yields

$$\text{one in the third term} = 4(2\pi)^3\delta^{(3)}(\vec{k_1}+\vec{k_2}+\vec{k_3}+\vec{k_4})P_{\mathcal{R}}(|\vec{k_3}|)P_{\mathcal{R}}(|\vec{k_4}|)\big[P_{\mathcal{R}}(|\vec{k_1}+\vec{k_3}|)+P_{\mathcal{R}}(|\vec{k_1}+\vec{k_4}|)\big].$$

By combining all individual results, the four-point function is

$$\begin{aligned}\big\langle\mathcal{R}(\vec{k_1})\mathcal{R}(\vec{k_2})\mathcal{R}(\vec{k_3})\mathcal{R}(\vec{k_4})\big\rangle =&(2\pi)^3\Big\{\delta^{(3)}(\vec{k_1}+\vec{k_2})\delta^{(3)}(\vec{k_3}+\vec{k_4})P_{\mathcal{R}}(|\vec{k_1}|)P_{\mathcal{R}}(|\vec{k_3}|)+\text{perm}(2,3,4)\Big\}\\
&+(2\pi)^3\delta^{(3)}(\vec{k_1}+\vec{k_2}+\vec{k_3}+\vec{k_4})\Big\{\\
&\frac{54}{25}g_{NL}\Big[P_{\mathcal{R}}(|\vec{k_1}|)P_{\mathcal{R}}(|\vec{k_2}|)P_{\mathcal{R}}(|\vec{k_3}|)+\text{perm}(1,2,3,4)\Big]\\
&+\frac{36}{25}f_{NL}^2\Big[P_{\mathcal{R}}(|\vec{k_3}|)P_{\mathcal{R}}(|\vec{k_4}|)\big[P_{\mathcal{R}}(|\vec{k_1}+\vec{k_3}|)+P_{\mathcal{R}}(|\vec{k_1}+\vec{k_4}|)\big]+\text{perm}(1,2,3,4)\Big]\Big\}.\end{aligned}$$

The results here is the same one as (7.0.1) but for the single-field model only. The peak limits of it are discussed in the section 7 where the multi-field consistency (7.0.5) arises. In this case, the parameter τ_{NL} is at its minimum, $\tau_{NL}=\left(\frac{6}{5}f_{NL}\right)^2$. In the multi-field scenarios, it is more intuitive to compute via the δN-*formalism* [23–25]. The computation there will give the multi-field consistency relation (7.0.5): $\tau_{NL}\geq\left(\frac{6}{5}f_{NL}\right)^2$. The relation implies that the parameter in multi-field scenarios can become greater than the case of single-field computed here. The importance of this relation have been discussed in the section 7.